Rep. Prog. Phys. **50** (1987) 731–781. Printed in the UK

Large-scale nuclear structure studies

K W Schmid† and F Grümmer‡

† Universität Tübingen, Institut für theoretische Physik, D-7400 Tübingen, West Germany
‡ Kernforschungsanlage Jülich GmbH, Institut für Kernphysik, D-5170 Jülich, West Germany

Abstract

The problem of microscopic nuclear structure theory in large single particle basis systems is reviewed. Several approaches are discussed, which attempt to approximate the large model spaces numerically inaccessible in complete shell model expansions of the nuclear wavefunctions. All of them use symmetry projected Hartree-Fock-Bogoliubov quasiparticle configurations as basic building blocks of the theory. They differ, however, in the degree of sophistication of the variational procedures which are used to determine the corresponding mean fields as well as the configuration mixing, up to a level, on which the construction of the configuration space itself is entirely left to the dynamics of the considered system. The mathematical formalism underlying these models is briefly summarised and the steps towards a numerical realisation are discussed. In several examples the possibilities and the power of the models are demonstrated and their limitations are shown. The models may provide a powerful tool for the analysis of experimental data as well as for predictions in still unexplored regions. On the other hand they may lead to a much better theoretical understanding of effective nuclear interactions as well as the underlying fundamental forces.

This review was received in November 1986.

0034-4885/87/060731+51$09.00

Contents

1. Introduction

Being a complex composite system of many constituents, the nucleus displays a multitude of various excitations, which may be classified by their constants of motion: energy, angular momentum, parity and at least in light systems also the total isospin. The energetically lowest state of each angular momentum is usually called the yrast state, and the higher ones are referred to as non-yrast excitations. Both yrast as well as non-yrast states may be either of single particle or of collective nature according to the number of constituents taking part in the particular excitation. Furthermore, we usually distinguish between the nuclear continuum, being high enough in excitation energy so that a decay via nucleon (or even nucleus) emission is possible, and the discrete levels lying below the emission threshold for hadronic particles and hence being able to decay only by photon emission (or electron conversion) into the energetically lower states of the same or, for example, by β decay of neighbouring nuclear systems.

To explore these discrete excitations and their measurable properties all over the nuclear mass table is the classical field of experimental nuclear spectroscopy; to explain the complex interplay of collective and single particle degrees of freedom causing these properties is the central aim of theoretical nuclear structure physics.

Within the last decade experimental nuclear spectroscopy has been rapidly developing. Many powerful tools and methods leading to a flood of new data all over the nuclear mass table have been created. Only a few of them can be mentioned here.

Measurements of multiple γ coincidences following heavy ion fusion reactions with sophisticated Compton suppressed detector arrays (Twin *et al* 1984, Leider *et al* 1984, Stephens 1985) have explored the yrast bands of many nuclei up to very high angular momentum (Twin *et al* 1986) and also revealed very complex patterns of non-yrast side bands up to an almost 'complete spectroscopy' below a certain excitation energy in particular nuclei (Haque *et al* 1985). Furthermore, the method of transient fields has opened up new possibilities to investigate the magnetic properties of rather short-lived states (Benczer-Koller *et al* 1980) and refinements of the Coulomb excitation and lifetime measurements allowed to extract rather accurate quadrupole moments and transition probabilities in many individual cases (see, e.g., Emling 1984). Last, but not least, inelastic electron scattering has provided extremely precise information about the detailed structure of many nuclear excitations (Heisenberg and Blok 1983).

The classification and interpretation of this enormous amount of new data has been a serious challenge to theoretical nuclear structure physics and indeed led to a rapid development of rather successful methods. So, for example, the cranked shell model (CSM) approach (Bengtsson and Frauendorf 1979) describing the nucleus as a system of independent nucleons moving in a phenomenologically chosen deformed rotating mean field was able to explain a lot of high spin phenomena in a rather simple and intuitive way. On the other hand the nculeus has been viewed as a system of boson-like nucleon pairs coupled to low angular momenta (usually only 0 and 2) and interacting via a simple phenomenological Hamiltonian. This interacting boson approximation (IBA), first introduced by Arima and Iachello (1975a, b), with its countless extensions developed since then has, in particular, yielded an almost surprisingly good description

of the excitation energies of many yrast and non-yrast states in various mass regions with actually very few parameters (Arima and Iachello 1984).

However, all these phenomenological approaches have their natural limitations. So, for example, the CSM approach does not yield proper quantum mechanical wavefunctions and hence cannot be used to obtain quantitative information about electromagnetic transition probabilities or form factors. On the other hand the boson models, at least in their simpler versions, are not suitable for studying high spin phenomena, and last but not least both approaches perform rather poorly in light nuclei. This is actually no surprise since, for the sake of simplicity, all these models restrict themselves deliberately to only a few phenomenological variables claiming that these describe the essential degrees of freedom relevant for the particular excitations under consideration reasonably well. A real 'first principle' approach, however, should incorporate all the degrees of freedom simultaneously and leave it to the dynamics of the system itself, namely the interactions between its various constituents, to determine the relevant ones. Only such a microscopic nuclear structure model can be expected to yield a unified description of nuclear structure phenomena all over the mass table irrespective of their particular nature.

Unfortunately, even if we discard relativistic effects and subnucleonic degrees of freedom entirely and assume the traditional point of view to consider the nucleus as a system of interacting inert nucleons, an approximation which seems to be rather well justified restricting ourselves to low energy discrete excitations, the remaining conventional nuclear many body problem is still much too difficult to be treated in actual applications. The main obstacle is that the interaction between two nucleons inside the nucleus is not the same as the free interaction encountered by two nucleons in the vacuum but is renormalised due to the presence of the other nucleons, which block part of the phase space available in the free scattering (Pauli blocking). The details of this renormalisation, however, depend on the structure of the nuclear medium, which in turn results from the renormalised interaction, and so on. Thus we actually encounter two many body problems, one for the effective interaction and one for the nuclear structure, which are intimately connected and hence, at least in principle, should be solved simultaneously by some self-consistent procedure. To complicate the problem even more, the effective many body Hamiltonian acts in the full infinite Hilbert space, while for practical solutions of the many body Schrödinger equation in most cases the use of finite model spaces is required. Though seeming again to be rather well justified for the particular problem of low lying discrete excitations, the restriction to a finite model space, however, introduces further renormalisations of the effective Hamiltonian, which are to be determined by yet another self-consistent procedure.

Being unable to solve this highly complex non-linear problem, in practice one usually separates the force and the nuclear structure problems from each other and simply assumes that for the chosen model space the appropriate effective many body Hamiltonian is given. At least in principle then, the remaining problem becomes trivial and 'all' that is left to be done is the diagonalisation of the given Hamiltonian in the complete (finite) space of A nucleon configurations constructable in the chosen model space. This is the so-called complete shell model configuration mixing (SCM) approach to the nuclear many body problem (Halbert *et al* 1971, Whitehead *et al* 1977, Brussaard and Glaudemans 1977, McGrory and Wildenthal 1980). This method has the big advantage of allowing for a direct comparison with many experimental data and thus, being exact under the above assumptions, to yield rather valuable information about the deficiencies of the underlying effective Hamiltonian itself. In fact, if enough

experimental data are available, the effective Hamiltonian appropriate for the chosen model space can even be determined empirically by least square fit procedures (e.g. Chung 1976), a method, which by comparing its results to those of more fundamental attempts to determine the interaction (e.g. Kuo and Brown 1968), has helped to improve our microscopic understanding of effective forces in nuclei considerably. Thus, although seeming at first, in the light of the above discussion, to be as artificial as an answer to the question of which was first, egg or hen, the separation of the force and the nuclear structure many body problems turns out to be a rather reasonable simplification of the full problem.

Unfortunately, the number of A nucleon configurations to be treated increases dramatically with the number of single particle states defining the model space. Thus complete SCM calculations, being referred to as the only real 'large-scale' nuclear structure studies for a very long time, are actually restricted to rather 'small-scale' model spaces (typically of the size of, for example, the 1s0d shell), and consequently this method is limited to a very small class of nuclear excitations. In fact, even such apparently simple tasks as the description of negative parity states in light doubly even nuclei are already beyond its possibilities, to say nothing about the spectroscopy of medium heavy and heavy nuclei, where even more single particle orbits are expected to contribute already for the low lying positive parity excitations.

Thus for most nuclear structure problems the complete SCM expansion of the nuclear wavefunction has to be truncated drastically, and the question of how this truncation can be performed in order to account for a maximum of the correlations in the considered system via as few as possible A nucleon configurations is the central problem of all microscopic nuclear structure applications in large model spaces.

The most extreme case of such a truncation is provided by the so-called mean field approaches like the Hartree-Fock (HF) (Hartree 1928, Fock 1930) or the more general Hartree-Fock-Bogoliubov (HFB) theory (Bogoliubov 1958, 1959, Bogoliubov and Soloviev 1959, Valatin 1961) viewing the nucleus as a system of independent quasiparticles moving in an 'optimal' average potential, which is extracted directly from the effective many body Hamiltonian via a variational procedure. Both methods have actually been well established in nuclear physics for a long time (see, e.g., Kelson 1963, Ripka 1968, Baranger 1961, 1963a, b, respectively) and indeed have been used rather successfully for the description of the ground-state properties of many nuclei in large single particle basis systems (e.g. Decharge and Gogny 1980). Since the resulting mean fields furthermore account for much more correlations than the *ad hoc* chosen basis-creating potential used in the SCM method, it seems to be rather attractive to use the corresponding HF or HFB ground state as a reference for the construction of a truncated configuration space to be used as a basis for the diagonalisation of the many body Hamiltonian.

However, already the mean field approaches themselves encounter a serious complication: intimately connected with the ability of, for example, the HFB approach to account for a large part of the complete SCM expansion of the ground state via a single configuration is its non-conservation of certain symmetries, which are required by the many body Hamiltonian, such as for example, angular momentum and particle number. Thus the HFB solution as such cannot yet be considered as a physical state but only as some intrinsic structure, from which the components with the required symmetries are still to be obtained with the help of complicated projection techniques. Furthermore, in order to obtain really optimal solutions for any set of simultaneously conserved quantum numbers separately, this restoration of the broken symmetries

should be performed before the mean field is determined via a variational calculation. For a long time this was only possible by imposing rather restrictive approximations on the projection operator, as was done for example in the self-consistent cranking approach developed and applied mainly by the Munich group (see, e.g., Mang 1975). However, this approach leads to similar difficulties as already mentioned for its 'pedestrian brother', the CSM approach, and will hence not be discussed here any further. The situation becomes even worse if one tries to extend the mean field approaches into multiconfiguration methods, using, for example, a set of general HFB-type quasiparticle configurations as a many particle basis system. Then, in order to avoid spurious effects due to the linear dependences in this basis with respect to the symmetry operators, the restoration of the broken symmetries before the diagonalisation of the many body Hamiltonian even becomes compulsory.

In spite of these difficulties, in the last few years considerable progress has been made in this direction, and it will be these methods somewhere in between the pure mean field theories and a full SCM description which will be reviewed in the present article.

Using HF mean fields and projected one particle-one hole configurations, first attempts along these lines had already been made some years ago (Schmid and DoDang 1977, 1978, Schmid 1981). For the case of HFB mean fields and projected two quasiparticle configurations Hara and Iwasaki (1979, 1980) presented a similar model. However, their approach was restricted to rather special types of interactions and thus had only a limited range of applicability. A more general concept of such theories as well as a whole hierarchy of various possible approximations was then presented by Schmid *et al* (1984a). All the approaches discussed there use symmetry projected HFB type quasiparticle determinants as basic ingredients; however, they differ by the degree of sophistication of the variational procedures being used to determine the underlying mean fields as well as the configuration mixing degrees of freedom. In the meantime all these models have been numerically realised, except for one, up to finally reaching a level on which the construction of the configuration space itself is entirely left to the dynamics of the considered system and determined by a chain of successive variational calculations. Furthermore, all these approaches can handle arbitrary general two body interactions and, unlike the SCM method, can be applied in rather large model spaces. Thus they allow for the first time 'large-scale' nuclear structure studies going far beyond the possibilities of the SCM description to be performed.

As it is concerned with such recent developments, the present article obviously cannot be expected to resemble a review about an almost closed field. Instead, it naturally has to become a sort of status report on what has been achieved and what still has to be done. Thus, instead of giving a complete survey about all the various applications, we shall put the emphasis on a careful elaboration of the different approaches, illustrated by representative results, and give an extensive discussion about their individual achievements and drawbacks. In this way we also hope to avoid the obvious danger of being carried away by our own euphoria and being forced to review almost entirely our own work, since at least at present alternative approaches are not available.

2. General theoretical tools

In this section we shall briefly sketch the most exact approximation to the microscopic

description of discrete nuclear states within finite model spaces, namely the above-mentioned complete SCM approach. Unfortunately, as we shall see by simple counting of the number of configurations to be handled, this approach is restricted to single particle basis systems, which are much smaller than required by most nuclear structure problems. Thus being forced to develop suitable truncation schemes, we shall be led into the so-called mean field approaches, the most general of them being the HFB theory, which will serve as a starting point for all the various approaches to be discussed in the present article. We shall then demonstrate how number conservation and rotational symmetry can be restored from general HFB type many quasiparticle configurations, and finally we shall explain how the matrix elements of general operators between such projected configurations can be evaluated. All this will be presented in a rather brief manner giving always only the essentials of the formalism and leaving the interested reader to refer to the original publications for details.

2.1. The 'exact' approach to the nuclear many body problem

As already mentioned in the introduction we shall base our discussion throughout the present article on two fundamental assumptions.

(1) We shall assume that for a satisfactory description of most discrete nuclear excitations the use of a finite model space is sufficient. We define this model space by an M-dimensional set of orthonormal spherical single nucleon states $\{|i\rangle, |k\rangle, \ldots\}_M$, for example eigenstates $|i\rangle = |\tau nljm\rangle$ of a harmonic oscillator Hamiltonian with spin-orbit coupling. The corresponding creation and annihilation operators will be denoted by $\{c_i^+, c_k^+, \ldots\}_M$ and $\{c_i, c_k, \ldots\}_M$, respectively. They fulfil the usual anticommutation relations for fermion operators. The corresponding particle vacuum $|0\rangle$ is defined by $c_i|0\rangle \equiv 0$ for all $i = 1, \ldots, M$.

(2) We shall furthermore assume that the effective many body Hamiltonian appropriate for this model space is known and can be written in the chosen representation as a sum of one and two body terms only

$$\boldsymbol{H} = \sum_{uk} t(ik) c_i^+ c_k + \tfrac{1}{4} \sum_{ikrs} v(ikrs) c_i^+ c_k^+ c_s c_r. \tag{2.1}$$

Here $t(ik) \equiv \langle i|\boldsymbol{t}|k\rangle$ and $v(ikrs) \equiv \langle ik|\boldsymbol{V}|rs - sr\rangle$ are shorthand notations for the one body matrix elements and the antisymmetrised two body matrix elements of the effective interaction, respectively. The $t(ik)$ are in general the matrix elements of the kinetic energy operator (possibly renormalised) or, if an inert core of nucleons is assumed, some suitably chosen single particle energies. For the $v(ikrs)$ either a phenomenological ansatz may be used or they can be obtained on a more fundamental basis, for example from some reaction G matrix (see, e.g., Kuo and Brown 1968).

For the remaining A nucleon problem being subject to these two approximations a complete basis of configurations can be easily obtained by distributing the N neutrons and Z protons in all possible Pauli-allowed ways over the available M_n neutron and M_p proton orbits ($M_n + M_p = M$), respectively. That means we have to construct all Slater determinants

$$\left\{ |NZ_s\rangle = \prod_{\nu=1}^{N} c_{i_\nu}^+ \prod_{\mu=1}^{Z} c_{i_\mu}^+ |0\rangle;\ s = 1, \ldots, n \right\} \tag{2.2}$$

where $s = 1, \ldots, n$ labels all the possible occupations. Diagonalising the full Hamiltonian (2.1) in the complete basis (2.2) then yields the exact SCM solutions for our

restricted problem. In general n has the value

$$n = \binom{M_p}{Z}\binom{M_n}{N}.$$

By making use of the symmetries of (2.1), however, this number can be drastically reduced. So for example with (2.1) being parity conserving, (2.2) can obviously be split into two different subspaces, each of them containing only Slater determinants with a definite parity. Furthermore, using the fact that the Hamiltonian (2.1) commutes with the z component of the total angular momentum J_z, it is sufficient to consider the Slater determinants which are eigenstates of J_z with the eigenvalue $K = 0$ for even-even or odd-odd systems, while for odd systems only the $K = \frac{1}{2}$ configurations have to be taken into account. This is the so-called 'm-scheme' being used for example in the Glasgow shell model code (Whitehead *et al* 1977).

A further reduction of the number of configurations to be actually treated in the diagonalisation can be obtained by always coupling several of the Slater determinants (2.2) to a single configuration α being an eigenstate of the total angular momentum (eigenvalue I) and its z component (eigenvalue K) simultaneously. This yields configuration spaces of the type

$$\left\{ |NZIK;\alpha\rangle = \sum_{s=1}^{n} |NZs\rangle\langle NZs|NZIK;\alpha\rangle;\ \alpha = 1, \ldots, n(I) \leqslant n \right\} \tag{2.3}$$

where α subsumes all the relevant quantum numbers, which are not explicitly indicated, and $n(I)$ is usually much smaller than n. For charge symmetric Hamiltonians such a coupling can also be performed for the total isospin quantum numbers and hence a further reduction of the dimensions of the subspaces (2.3) can be reached. This method is used for example in the Oak Ridge-Rochester (Halbert *et al* 1971, McGrory and Wildenthal 1980) and Utrecht (Brussaard and Glaudemans 1977) formulations of the shell model problem.

Unfortunately, even in the latter representation, the number of configurations increases drastically with the number M of basis orbitals to be taken into account. Table 1 shows as an example the dimensions of the $I^\pi = 0^+$ subspaces (2.3) for three selected doubly even nuclei in various basis systems.

It is easily seen from these numbers that complete SCM calculations in not even very large basis systems are not only impracticable but plainly impossible. Coupling the configurations (2.3) in addition to good total isospin T does not improve this situation significantly. In general only about one order of magnitude can be gained. For example, there are already 839 $T = 0$ configurations among the 3372 $I^\pi = 0^+$ states

Table 1. Total number of isospin uncoupled $I^\pi = 0^+$ shell model configurations for the three nuclei ^{12}C, ^{20}Ne and ^{28}Si in different basis systems, which are defined by the quantum numbers of the included single particle orbits. 0p means e.g. the inclusion of the nlj = 0p1/2 and 0p3/2 orbits. If only one spin-orbit partner is included, the j value is explicitly given.

basis →	(1s0d)	(0p1s0d)	(0s0p1s0d)	(0s0p1s0d1p0f)	(0s0p1s0d1p0f0g9/2)
^{12}C	—	24 790	2 936 582	11 384 214 614	103 067 319 600
^{20}Ne	46	2984 286	51 475 358	312 959 701 138 592	23 093 317 425 235 138
^{28}Si	3372	627 558	2 936 582	175 864 552 746 785 562	136 124 437 576 139 270 616

for ^{28}Si in the 1s0d basis and the 1.36×10^{20} $I^\pi=0^+$ configurations in the (0s0p1s0d1p0f0g9/2) basis still contain 1.22×10^{19} $T=0$ states.

It should be stressed here that the basis systems listed in table 1 are far from being unphysically large. So for example the description of the low energy spectrum of medium heavy and heavy nuclei requires the use of model spaces, which are at least of comparable size to the larger systems listed in the table, and even for such comparatively simple tasks as the description of negative parity states in doubly even 1s0d shell nuclei at least a (0p1s0d1p0f) basis would be needed, to say nothing about problems like the description of the electric quadrupole transition strength distribution in open-shell nuclei, where at least five major shells for both protons and neutrons should be taken into account.

Thus, for most problems of nuclear structure physics, we are forced to truncate the complete SCM expansion of the nuclear wavefunctions drastically in order to be left with a numerically manageable number of configurations. One could try to restrict the diagonalisation to a certain subset of (2.3) selecting the configurations according to their unperturbed energies. Indeed such n-$\hbar\omega$ truncation schemes (using all configurations within one major shell, but only the two particle-two hole (2p2h) excitations leading to the next and only the 1p1h configurations connecting with the overnext shell would, for example, be a 2-$\hbar\omega$ truncation) have been recently investigated (Glaudemans 1985), and their first results are at least partly rather encouraging. However, it has also become clear that such schemes lead into serious convergence problems at least for such states in the nuclear spectrum which are of a more collective nature.

In the present article we shall not comment on this type of approach any further. Instead we shall turn our attention to another type of truncation scheme, in which the selection of the configurations is not done 'by hand' but guided by the dynamics of the considered system itself. The basic idea is to use variational principles in order to extract directly from the Hamiltonian the optimal mean field each of the nucleons feels due to its interaction with all the others. The total wavefunctions are then to be expanded around this optimised mean field instead of taking some arbitrary basis-creating potential as is done in the SCM method.

2.2. Mean fields and quasiparticles: the general concept

Mathematically any mean field can be introduced by a set of quasiparticles being defined by a linear transformation of the particles and holes of the chosen single particle basis. The most general quasiparticles to be obtained have, therefore, the form

$$a_\alpha^+=\sum_{i=1}^{M}\left(A_{i\alpha}c_i^+ + Bi_\alpha c_i\right) \qquad \alpha=1,\ldots,M \tag{2.4}$$

or, in more elegant matrix notation,

$$\begin{pmatrix} a^+ \\ a \end{pmatrix} = F\begin{pmatrix} c^+ \\ c \end{pmatrix} \equiv \begin{pmatrix} A^{\mathrm{T}} & B^{\mathrm{T}} \\ B^+ & A^+ \end{pmatrix}\begin{pmatrix} c^+ \\ c \end{pmatrix} \tag{2.5}$$

with F being restricted to be a unitary $(2M\times2M)$ matrix

$$F^+F=FF^+=\mathbf{1} \tag{2.6}$$

in order to ensure fermion anticommutation relations for the quasiparticle operators, too. Equation (2.5) and (2.6) define a general HFB transformation F.

It has been shown (Bloch and Messiah 1962, Zumino 1962) that any transformation of the type (2.5) can be decomposed into three successive transformations

$$F=\begin{pmatrix} C^{\mathrm{T}} & 0 \\ 0 & C^{+} \end{pmatrix}\begin{pmatrix} U^{\mathrm{T}} & V^{\mathrm{T}} \\ V^{+} & U^{+} \end{pmatrix}\begin{pmatrix} D^{\mathrm{T}} & 0 \\ 0 & D^{+} \end{pmatrix}. \tag{2.7}$$

The first of these, D, obviously does not mix particles and holes and thus describes mean fields of the less general HF type. The second is a sort of BCS transformation (Bardeen *et al* 1957) which incorporates correlations between pairs of particles in the mean field. The third transformation, C, finally ensures an unambiguous representation of the quasiparticle operators.

The vacuum for the quasiparticle annihilators has the form

$$|F\rangle=\prod_{\alpha}^{M} a_{\alpha}(F)|0\rangle \tag{2.8}$$

where the label F has been introduced to indicate that the vacuum as well as the quasiparticle operators refer to a particular transformation (2.5).

It is immediately seen from (2.5) that the vacuum $|F\rangle$ is not an eigenstate of the particle number operator, but contains (for M even, as is always the case if all magnetic substates of the various spherical orbits are included) components with $0, 2, \ldots, M$ particles. The same holds for all configurations obtained from (2.8) by the application of an even number of quasiparticle creators (2.4). On the other hand any configuration being created via an odd number of creators will be a mixture of all odd nuclei ($1 \leqslant A \leqslant M-1$) contained within the chosen model space. This property of HFB type quasiparticle determinants is known as their number parity (Mang 1975).

The set of all number parity even determinants

$$\begin{aligned} &|F\rangle \\ &|\alpha\beta(F)\rangle \equiv a_{\alpha}^{+}(F)a_{\beta}^{+}(F)|F\rangle \\ &|\alpha\beta\gamma\delta(F)\rangle \equiv a_{\alpha}^{+}(F)a_{\beta}^{+}(F)a_{\gamma}^{+}(F)a_{\delta}^{+}(F)|F\rangle \\ &\quad\vdots \end{aligned} \tag{2.9}$$

forms a complete orthonormal basis for all the even mass nuclei within the chosen model space, while the set of all odd quasiparticle excitations

$$\begin{aligned} &|\alpha(F)\rangle \equiv a_{\alpha}^{+}(F)|F\rangle \\ &|\alpha\beta\gamma(F)\rangle \equiv a_{\alpha}^{+}(F)a_{\beta}^{+}(F)a_{\gamma}^{+}(F)|F\rangle \\ &\quad\vdots \end{aligned} \tag{2.10}$$

contains the complete SCM basis spaces (2.2) for all accessible odd mass systems.

Diagonalising the Hamiltonian in the complete spaces (2.9) and (2.10) is therefore equivalent to a solution of the SCM problem out of the last section for all even or odd nuclei simultaneously, and thus numerically even much less feasible. Furthermore, the results of such complete diagonalisations would obviously not depend at all on the particular choice of the unitary transformation F, and thus the introduction of the quasiparticles (2.5) seems somehow superfluous.

The situation changes, however, if only a limited number of configurations is going to be used in the actual calculation. Let us assume that we have chosen a particular set

$$\zeta \equiv \{|Q_1(F_1)\rangle, \ldots, |Q_{n_1}(F_1)\rangle, \ldots, |Q_1(F_m)\rangle, \ldots, |Q_{n_m}(F_m)\rangle\} \tag{2.11}$$

with always n_i different quasiparticle determinants of either the type (2.9) or (2.10) being based on a HFB transformation F_i allowing altogether for m different transformations. This is the most general ansatz for a configuration space built by in this case even non-orthogonal HFB type determinants with a given number parity. If (2.11) does not span the complete space, and this will always be assumed in the following, then the results obtained using ζ as a basis will obviously depend on the m transformations F_i as well as on the configuration mixing. These degrees of freedom can hence be used to maximise the amount of internucleon correlations to be accounted for in this truncated space. In fact, there will exist at least one optimal set of m HFB transformations and corresponding configuration mixing coefficients yielding a minimum of the total energy with ζ being used as model space in a variational calculation. In the extreme case that ζ includes only the vacuum $|F\rangle$ for one transformation such a procedure would coincide with the standard HFB theory.

The reason that with the general ansatz (2.11) a much deeper energy minimum can usually be reached than with any subset of the Slater determinants (2.2) including the same number of configurations is due to the fact that each of the configurations in (2.11) is already a rather complicated linear combination of many Slater determinants of the type (2.2). With the fields F_i and the configuration mixing used as variational degrees of freedom, these linear combinations can be optimised and thus a large part of the correlations induced by the Hamiltonian can be taken into account.

However, intimately connected to such attempts to account for as much as possible of the correlations via as few as possible configurations is a common price to be paid: the truncated space is not only incomplete with respect to the Hamiltonian but also for other operators commuting with the latter, and thus in (2.11) the corresponding symmetries will be broken. In general neither the angular momentum nor the particle number, neither the parity nor the total isospin are conserved. Hence the configurations (2.11) cannot be considered as physical configurations but only as some intrinsic structures, from which the many particle states with the desired quantum numbers are still to be obtained with the help of projection techniques. How, in practice, this restoration of the broken symmetries can be achieved will be discussed in the next section.

2.3. Restoration of broken symmetries

The techniques to restore the broken rotational symmetry (Peierls and Yoccoz 1957, Villars 1966) and the number conservation (Bayman 1960) from general HFB type quasiparticle determinants have been well known for a long time and have only recently been discussed by us rather extensively (Schmid *et al* 1984a).

Each quasiparticle determinant $|Q(F)\rangle$ can be formally expanded into the complete set of symmetry conserving shell model configurations (2.3)

$$|Q(F)\rangle = \sum_{NZIK\alpha} |NZIK;\alpha\rangle\langle NZIK;\alpha|Q(F)\rangle. \tag{2.12}$$

Thus, by applying the operator

$$\boldsymbol{P}(NZIM;K) \equiv \sum_{\alpha} |NZIM;\alpha\rangle\langle NZIK;\alpha| \tag{2.13}$$

onto (2.12)

$$\begin{aligned}\boldsymbol{P}(NZIM;K)|Q(F)\rangle &= \sum_{\alpha} |NZIM;\alpha\rangle\langle NZIK;\alpha|Q(F)\rangle \\ &\equiv |Q_K^{NZIM}(F)\rangle\end{aligned} \tag{2.14}$$

one obtains immediately a set of eigenstates of the particle number operators $\boldsymbol{N}$ and $\boldsymbol{Z}$ as well as of the square of the total angular momentum and its z component in the laboratory frame of reference. Note that (2.14) still depends on the orientation of the intrinsic quantisation axis via the different K components. The most general wavefunction to be obtained from a single determinant $|Q(F)\rangle$ has, therefore, the form

$$|Q^{NZIM}(F)\rangle = \sum_{K=-I}^{+I} |Q_K^{NZIM}(F)\rangle f_K^{NZI} \tag{2.15}$$

with the mixing coefficients f still to be determined dynamically in order to get rid of this unphysical orientation dependence. Thus in general already the projection of a single quasiparticle determinant introduces a set of additional variational parameters into the theory.

In practice the decomposition (2.12) is uaually not known. Then the integral representation of the operator (2.13) has to be used, which is given by

$$\begin{aligned}\boldsymbol{P}(NZIM;K) &= \frac{2I+1}{32\pi^4}\int \mathrm{d}\Omega\, \mathrm{d}\varphi_\mathrm{p}\, \mathrm{d}\varphi_\mathrm{n} D^{I*}_{MK}(\Omega) \exp(\mathrm{i}\varphi_\mathrm{p} Z)\exp(\mathrm{i}\varphi_\mathrm{n} N)\\ &\quad\times \boldsymbol{R}(\Omega)\exp(\mathrm{i}\varphi_\mathrm{p} Z)\exp(-\mathrm{i}\varphi_\mathrm{n} N)\\ &\equiv \int \mathrm{d}\tilde{\Omega}\, \omega^{NZI*}_{MK}(\tilde{\Omega})\tilde{\boldsymbol{R}}(\tilde{\Omega}).\end{aligned} \tag{2.16}$$

Here $\boldsymbol{R}(\Omega)$ is the usual rotation operator and $D^I_{MK}(\Omega)$ its representation in angular momentum eigenstates (Edmonds 1957). Ω subsumes the integrations over the full range of the three Euler angles and the integrations for the particle numbers both run from 0 to 2π. The definition of the generalised rotation $\tilde{\boldsymbol{R}}(\tilde{\Omega})$ and the corresponding weight function ω are obvious.

Using (2.16) the reduced matrix elements of any arbitrary tensor operator $\boldsymbol{T}^L_\mu(\Delta N, \Delta Z)$, which may even change the proton and neutron numbers by ΔN and ΔZ, respectively, in between arbitrary projected configurations (2.14), which may be based even on different quasiparticle transformations F_1 and F_2, can be calculated. One obtains

$$\begin{aligned}\langle Q^{N'Z'I'}_{1K'}(F_1)\|\boldsymbol{T}^L(\Delta N,\Delta Z)\|Q^{NZI}_{2K}(F_2)\rangle &= (2I'+1)^{1/2}\\ &\quad\times\sum_{\mu=-L}^{+L}(ILI'|K'-\mu\mu K')\int \mathrm{d}\tilde{\Omega}\,\omega^{NZI*}_{K'-\mu K}(\tilde{\Omega})\\ &\quad\times\langle Q_1(F_1)|\boldsymbol{T}^L_\mu(\Delta N,\Delta Z)\tilde{\boldsymbol{R}}(\tilde{\Omega})|Q_2(F_2)\rangle\end{aligned} \tag{2.17}$$

where the reduced matrix element is defined using Edmonds' (1957) convention.

If, in addition to number conservation and rotational symmetry, the parity is also broken, then we have to use instead of $|Q(F)\rangle$ the linear combinations

$$|Q^\pi(F)\rangle \equiv \tfrac{1}{2}[|Q(F)\rangle + \pi\boldsymbol{\Pi}|Q(F)\rangle] \tag{2.18}$$

in the above formulation. Here $\boldsymbol{\Pi}$ is the parity operator and $\pi = \pm 1$ are its eigenvalues.

Isospin projection will not be treated in the present review. In principle it can be incorporated using the same methods as for the angular momentum. However, some care has then to be taken with the number projections. In fact, projecting on both N and Z separately fixes the 3-component of the isospin in the intrinsic isospin frame (analogous to taking into account only a single K component in (2.15)) and thus does not yield the most general solution. For the case of a full isospin projection therefore the number conservation should only be restored for the total number of nucleons.

Now left to be considered is the rotated matrix element in (2.17). The special techniques needed for its evaluation will be briefly reviewed in the following section.

2.4. Evaluation of general matrix elements

For the evaluation of (2.17) one has to know how the quasiparticle operators (2.5) of a given HFB transformation F_2 transform under the generalised rotation operator $\tilde{\boldsymbol{R}}(\tilde{\Omega})$ being introduced in (2.16). One obtains

$$\begin{aligned}\begin{pmatrix} b^+ & (F_2,\tilde{\Omega}) \\ b & (F_2,\tilde{\Omega}) \end{pmatrix} &= \tilde{\boldsymbol{R}}(\tilde{\Omega})\begin{pmatrix} a^+ & (F_2) \\ a & (F_2) \end{pmatrix}\tilde{\boldsymbol{R}}^+(\tilde{\Omega}) \\ &= \tilde{F}_2(\tilde{\Omega})\begin{pmatrix} c^+ \\ c \end{pmatrix} \\ &\equiv F_2\begin{pmatrix} \tilde{R}^{\mathrm{T}}(\tilde{\Omega}) & 0 \\ 0 & \tilde{R}^+(\tilde{\Omega}) \end{pmatrix}\begin{pmatrix} c^+ \\ c \end{pmatrix}\end{aligned} \tag{2.19}$$

where

$$(\tilde{R}(\tilde{\Omega}))_{ik} \equiv \langle i|\tilde{\boldsymbol{R}}(\tilde{\Omega})|k\rangle \qquad i,k=1,\ldots,M \tag{2.20}$$

is the representation of $\tilde{\boldsymbol{R}}(\tilde{\Omega})$ in the chosen spherical single particle basis. Using the inverse transformation of (2.5) one can express the rotated quasiparticle operators (2.19) in terms of the unrotated quasiparticle operators belonging to a different HFB transformation F_1. One obtains

$$\begin{aligned}\begin{pmatrix} b^+ & (F_2,\tilde{\Omega}) \\ b & (F_2,\tilde{\Omega}) \end{pmatrix} &= \tilde{F}_2(\tilde{\Omega})F_1^+\begin{pmatrix} a^+ & (F_2) \\ a & (F_2) \end{pmatrix} \\ &= \begin{pmatrix} A_{12}^{\mathrm{T}}(\tilde{\Omega}) & B_{12}^{\mathrm{T}}(\tilde{\Omega}) \\ B_{12}^+(\tilde{\Omega}) & A_{12}^+(\tilde{\Omega}) \end{pmatrix}\begin{pmatrix} a^+ & (F_1) \\ a & (F_1) \end{pmatrix}\end{aligned} \tag{2.21}$$

where the rotated transformation matrices are given by

$$\begin{aligned} A_{12}(\tilde{\Omega}) &= A_1^{\mathrm{T}}\tilde{R}(\tilde{\Omega})A_2 + B_1^+\tilde{R}^*(\tilde{\Omega})B_2 \\ B_{12}(\tilde{\Omega}) &= B_1^{\mathrm{T}}\tilde{R}(\tilde{\Omega})A_2 + A_1^+\tilde{R}^*(\tilde{\Omega})B_2 \end{aligned} \tag{2.22}$$

with A_1, B_1 and A_2, B_2 being the unrotated HFB transformation matrices for the transformations F_1 and F_2, respectively, as defined by (2.5).

Using this result as well as the generalised version (Mang 1975) of Thouless' (1960) theorem, we can then express the rotated vacuum $\tilde{\boldsymbol{R}}(\tilde{\Omega})|F_2\rangle$ in terms of the vacuum $|F_1\rangle$ and the corresponding quasiparticle operators. We obtain

$$|\tilde{F}_2(\tilde{\Omega})\rangle \equiv \tilde{\boldsymbol{R}}(\tilde{\Omega})|F_2\rangle = n_{12}(\tilde{\Omega})\exp\left(\tfrac{1}{2}\sum_{\alpha\beta} g_{\alpha\beta}^{12}(\tilde{\Omega})a_\alpha^+(F_1)a_\beta^+(F_1)\right)|F_1\rangle. \tag{2.23}$$

Here the antisymmetric matrix $g^{12}(\tilde{\Omega})$ is given by

$$g^{12}(\tilde{\Omega}) = B_{12}^*(\tilde{\Omega})[X^{12}(\tilde{\Omega})]^{\mathrm{T}} \tag{2.24}$$

with

$$X^{12}(\tilde{\Omega}) \equiv [A_{12}^+(\tilde{\Omega})]^{-1} \tag{2.25}$$

and the rotated overlap $n_{12}(\tilde{\Omega})$ can be calculated following Onishi and Yoshida (1966). The result is

$$n_{12}(\tilde{\Omega}) = \langle F_1 | \tilde{F}_2(\tilde{\Omega}) \rangle = (\det A^{+}_{12}(\tilde{\Omega}))^{1/2} \exp[-\mathrm{i}/2(\varphi_n M_n + \varphi_p M_p)]. \tag{2.26}$$

Obviously at this point a difficulty is encountered concerning the sign of the square root. One has to ensure that $n_{12}(\tilde{\Omega})$ is a continuous function of the involved rotation angles. Since in practice one uses finite differences between these angles there may occur ambiguities which are difficult to resolve. This problem has been recently solved by Neergard and Wüst (1983). They designed a method, which allows a unique determination of the sign of the square root, and has also been used succesfully in our numerical applications.

Using the above expressions we can now proceed to calculate the general rotated matrix element in (2.17). The procedure can be summarised as follows.

First the HFB configuration $|Q_1(F_1)\rangle$ is written down explicitly as some n-quasiparticle excitation with respect to the vacuum $|F_1\rangle$

$$|Q_1(F_1)\rangle = a^{+}_{\alpha_1}(F_1) \ldots a^{+}_{\alpha_n}(F_1)|F_1\rangle. \tag{2.27}$$

Obviously n may be zero. Then by (2.27) the vacuum $|F_1\rangle$ is meant. The same is then done with the help of (2.19) for the rotated state on the right-hand side of the matrix element. Here we obtain in general some rotated m-quasiparticle state

$$\tilde{\boldsymbol{R}}(\tilde{\Omega})|Q_2(F_2)\rangle = b^{+}_{\beta_1}(F_2, \tilde{\Omega}) \ldots b^{+}_{\beta_m}(F_2, \tilde{\Omega})|\tilde{F}_2(\tilde{\Omega})\rangle. \tag{2.28}$$

Then use is been made of the inverse transformation of (2.5), which allows us to express any arbitrary operator in the quasiparticle representation F_1 as

$$\boldsymbol{T}^{L}_{\mu}(\Delta N, \Delta Z) = \sum_{p,p'} \sum_{\substack{\gamma_1,\ldots,\gamma_p \\ \delta_1,\ldots,\delta_{p'}}} (\boldsymbol{T}^{L}_{\mu})^{pp'}_{\gamma_1 \ldots \gamma_p;\delta_1 \ldots \delta_{p'}} a^{+}_{\gamma_1}(F_1) \ldots a^{+}_{\gamma_p}(F_1) a_{\delta_1}(F_1) \ldots a_{\delta_{p'}}(F_1) \tag{2.29}$$

with the γ and δ running over all the M quasiparticle states and p,p' both running from 0 to some maximum number determined by the special form of the operator actually being considered. How the expansion (2.29) looks, e.g., for the Hamiltonian and for some other operators, has been presented in detail elsewhere (see, e.g., Ring and Schuck 1980, Schmid *et al* 1984a) and hence will not be repeated here.

Using (2.27)-(2.29) the evaluation of the rotated matrix elements in (2.17) can now be reduced to the calculation of expressions of the form

$$\begin{aligned} &\langle F_1 | a_{\alpha_1}(F_1) \ldots a_{\alpha_n}(F_1) a^{+}_{\gamma_1}(F_1) \ldots a^{+}_{\gamma_p}(F_1) a_{\delta_1}(F_1) \ldots a_{\delta_{p'}}(F_1) \\ &\qquad \times b^{+}_{\beta_1}(F_2, \tilde{\Omega}) \ldots b^{+}_{\beta_m}(F_2, \tilde{\Omega}) | \tilde{F}_2(\tilde{\Omega}) \rangle. \end{aligned} \tag{2.30}$$

Using (2.21) and (2.23) this can be done with the usual Wick's theorem (Wick 1950) for the vacuum $|F_1\rangle$ on both sides. However, one can also introduce a sort of generalised Wick's theorem and obtain the matrix element (2.30) as a sum over all possible fully contracted combinations composed of four elementary non-vanishing contractions. These are

$$\begin{aligned} &\langle F_1 | a_\alpha(F_1) a^{+}_\gamma(F_1) | \tilde{F}_2(\tilde{\Omega}) \rangle n^{-1}_{12}(\tilde{\Omega}) = \delta_{\alpha\gamma} \\ &\langle F_1 | a_\alpha(F_1) a_\delta(F_1) | \tilde{F}_2(\tilde{\Omega}) \rangle n^{-1}_{12}(\tilde{\Omega}) = g^{12}_{\delta\alpha}(\tilde{\Omega}) \\ &\langle F_1 | a_\alpha(F_1) b^{+}_\beta(F_2, \tilde{\Omega}) | \tilde{F}_2(\tilde{\Omega}) \rangle n^{-1}_{12}(\tilde{\Omega}) = X^{12}_{\alpha\beta}(\tilde{\Omega}) \\ &\langle F_1 | b^{+}_\beta(F_2, \tilde{\Omega}) b^{+}_{\beta'}(F_2, \tilde{\Omega}) | \tilde{F}_2(\tilde{\Omega}) \rangle n^{-1}_{12}(\tilde{\Omega}) = \tilde{g}^{12}_{\beta\beta'}(\tilde{\Omega}) \end{aligned} \tag{2.31}$$

where the antisymmetric matrix $\tilde{g}^{12}$ in the last expression is given by

$$\tilde{g}^{12}(\tilde{\Omega}) = B^{+}_{12}(\tilde{\Omega}) X^{12}(\tilde{\Omega}). \tag{2.32}$$

With the mathematical tools needed to calculate arbitrary matrix elements thus being available, we may now, fortunately, leave this rather formal discussion and turn for the rest of this review to the physically more interesting questions, namely how, in practice, suitable truncated configuration spaces of the type (2.11) can be chosen and the corresponding mean fields be determined.

3. Fixed mean field: the MONSTER(HFB) approximation

The simplest and therefore numerically first realised (Schmid *et al* 1984b) approach along the lines discussed above uses for all states of a considered nucleus a single fixed mean field which can be obtained by standard HFB theory. As configuration space for even mass systems then the projected vacuum as well as the projected two quasiparticle excitations with respect to it are taken. This approximation gave rise to the name MONSTER (model for handling many number- and spin-projected two quasiparticle excitations with realistic interactions and model spaces).

3.1. Formulation of the model and numerical approximations

In the standard HFB theory the mean field is obtained by requiring a minimum of the expectation value of the many body Hamiltonian within the vacuum configuration (2.8) with respect to variations of the HFB transformation matrix $\boldsymbol{F}$

$$\delta\langle F|\boldsymbol{H}-\sum_{\tau}\lambda_{\tau}\boldsymbol{N}_{\tau}|F\rangle=0 \tag{3.1}$$

where the constraints

$$\langle F|\boldsymbol{N}_{\tau}|F\rangle=N_{\tau} \qquad \tau=\mathrm{n},\mathrm{p} \tag{3.2}$$

are introduced in order to ensure that the required nucleon numbers are at least conserved on average.

For even mass nuclei the projected HFB vacuum and all, or at least the most important, projected two quasiparticle excitations with respect to it are taken into account

$$\zeta_{\mathrm{even}}(NZI)=\{\boldsymbol{P}(NZIM;K)|F\rangle,\boldsymbol{P}(NZIM;K)a_{\alpha}^{+}(F)a_{\beta}^{+}(F)|F\rangle;$$
$$K=-I,\ldots,+I;\ \alpha<\beta=1,\ldots,M\}. \tag{3.3}$$

Similarly we may define a truncated model space for odd systems consisting of all projected one quasiparticle excitations

$$\zeta_{\mathrm{odd}}(NZI)=\{\boldsymbol{P}(NZIM;K)a_{\alpha}^{+}(F)|F\rangle;\ K=-I,\ldots,+I;\ \alpha=1,\ldots,M\}. \tag{3.4}$$

The projected wavefunctions in both these model spaces are no longer orthonormal. Thus the variation of the total energy with respect to the mixing coefficients of the different configurations leads to a matrix equation of the type

$$(H-EN)f=0 \tag{3.5}$$

where H and N are the Hamiltonian and overlap matrices in the above configurations, respectively. The condition

$$f^{+}Nf=1 \tag{3.6}$$

ensures the orthonormality of the resulting many particle wavefunctions, which in the case of an even system have the general form

$$|\Psi_M^{NZI};\, a\rangle \equiv \sum_K \{\boldsymbol{P}(NZIM;\, K)|F\rangle f_{K0;a}^{NZI} + \sum_{\alpha<\beta} \boldsymbol{P}(NZIM;\, K) a_\alpha^+(F) a_\beta^+(F)|F\rangle f_{K\alpha\beta;a}^{NZI}\}. \tag{3.7}$$

Though being conceptually rather simple, the numerical realisation of this approach leads to tremendous complications, mainly because of the fivefold integration induced by the projection operator (2.16). However, the task can be considerably simplified, if in practical applications the most general HFB transformation (2.5) is not used but certain symmetries are imposed on the quasiparticles.

(1) The mixing of proton with neutron states in the quasiparticle transformation is neglected. Then the matrix F becomes real. Furthermore all the quasiparticle determinants can be written as a product of a neutron and a proton component. Physically this approximation is equivalent to the neglect of proton-neutron pairing correlations in the mean field.

(2) Parity mixing via the transformation (2.5) is not allowed. Consequently each quasiparticle configuration is an eigenstate of the parity operator.

(3) Finally, axial symmetry is enforced. Then the quasiparticle configurations are also eigenstates of the z component of the total angular momentum operator. In this case the integration over two of the three Euler angles involved in the angular momentum projection can be performed analytically.

In spite of the rather restrictive assumptions concerning the mean field, the configuration spaces and the symmetries of the quasiparticles, the MONSTER(HFB) approach is still a rather powerful model with a wide range of applicability. This will be illustrated in the following section.

3.2. Selected results of realistic applications

The quality of the MONSTER approach can be checked by comparing its results with those of complete SCM calculations. This is of course only possible in small model spaces. As an example we present here the results obtained for ^{22}Ne using the 1s0d shell as a single particle basis and a phenomenological many body Hamiltonian from the literature (Halbert *et al* 1971).

In figure 1 the results obtained for this nucleus with four different mean field approximations are compared with the exact SCM spectrum. Although in general the HFB mean field one obtains for ^{22}Ne has neutron pairing correlations, one can construct an unpaired mean field by restricting the HFB transformation (2.5) to the less general HF form (transformation D in (2.7)). By projecting the components with different angular momenta from the corresponding ground-state solution one obtains the leftmost spectrum. The second spectrum results from the projection of the full HFB vacuum. The next two spectra are obtained by admixing all one particle-one hole states to the HF vacuum, and all two quasiparticle excitations to the HFB mean field, respectively. One sees immediately that configuration mixing is essential in order to obtain the large number of states seen in SCM calculations, but also to obtain additional correlations in the ground-state band, which result in the well known deviations from the rotational behaviour. In particular, for low angular momenta pairing correlations turn out to be quite essential. One sees that the MONSTER approximation reproduces the exact SCM result for the ground band as well as many other excited states very nicely. On the

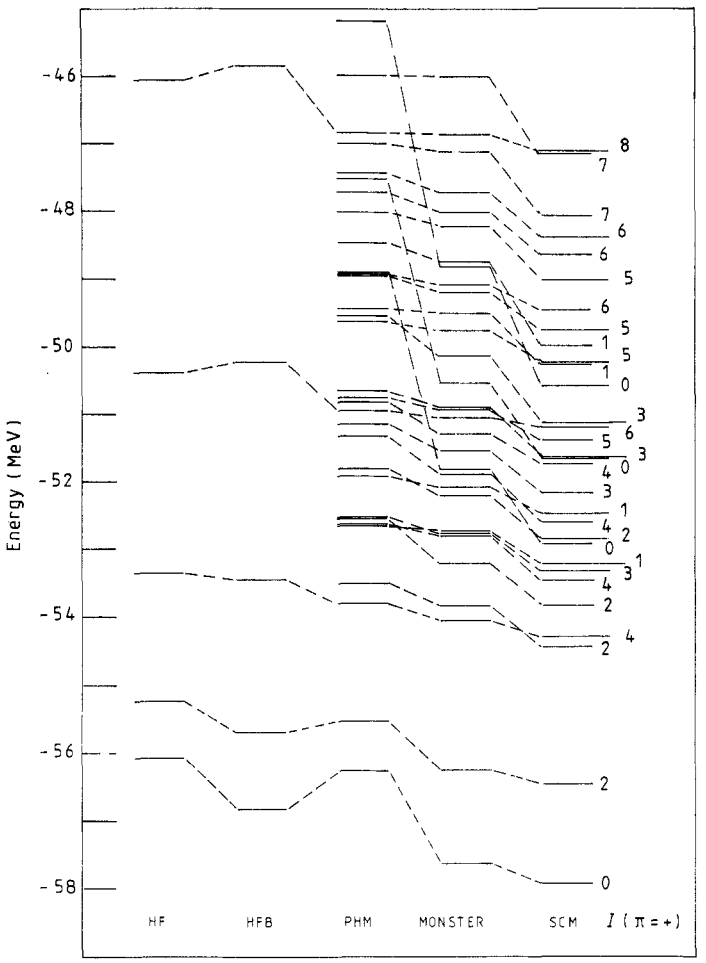

Figure 1. $T = 1$ states in ^{22}Ne: from left to right the following spectra are shown: projected HF, projected HFB, projected HF plus particle-hole excitations (PHM), MONSTER and SCM.

other hand there are some states, especially some excited 0^+ levels, which cannot be well described by any of the mean field approximations. They have obviously a more complicated structure than accounted for by the MONSTER configuration space, and we shall discuss later how one can improve upon their description. It is well known that one should not evaluate the quality of a wavefunction by just looking to the energies, since moments and, even more, non-diagonal quantities like transition probabilities are much more sensitive to details of the many body wavefunctions. We checked these quantities, too, and would like to mention here only the result that concerning moments and transitions the agreement of our approximate calculations with the exact results was also quite satisfactory. Thus we may conclude that the truncation scheme employed here is rather reasonable. This gives rise to the hope that also in larger model spaces a good approximation to the there non-accessible exact solutions is obtained.

As a second example we would like to demonstrate the applicability of the MONSTER to the description of high spin phenomena in heavy deformed nuclei. Many of those

nuclei display the so-called backbending effect, a sudden decrease of the observed γ transition energies within the yrast band at some critical angular momentum. This effect results from a complex interplay of the pairing correlations and the Coriolis force in the rotating frame of reference. The latter, being especially strong for nucleons in high-j single particle orbits, favours the breakup of a pair of particles and the alignment of their angular momenta along the axis of rotation. The ability of the MONSTER approach to describe this behaviour is demonstrated for the nucleus ^{164}Er. For this calculation a single particle basis consisting of the $N=4$ plus the $0h_{11/2}$ and $0h_{9/2}$ oscillator orbits for the protons and of the $N=5$ plus the $0i_{13/2}$ and $1g_{9/2}$ states for the neutrons has been used. The single particle energies have been taken from Kumar and Baranger (1968) and the effective interaction was an '*ad hoc*' chosen pairing plus quadrupole force including quadrupole pairing with the parameters given by Schmid *et al* (1984b). The spectrum has been slightly adjusted by the introduction of a constant effective moment of inertia for the core $\Theta_c = 5.8\ \mathrm{MeV}^{-1}$, which probably could have been avoided by a proper readjustment of the force parameters. The resulting ground and aligned bands are shown and compared with the experimental data in figure 2. The leftmost column in this figure shows the energies obtained from the angular momentum projected HFB vacuum. It is clearly seen that this HFB result already starts to deviate from the experimental spectrum at low spins. On the other hand the MONSTER yields a rather good description of the experimental excitation energies. The backbending phenomenon is even quantitatively well described.

Finally, in order to demonstrate the full power of the model, we shall present here some results of a systematic study of many nuclei in the $A=130$ mass region (Hammaren *et al* 1985, 1986a,b). This mass region had been chosen for several reasons. First of

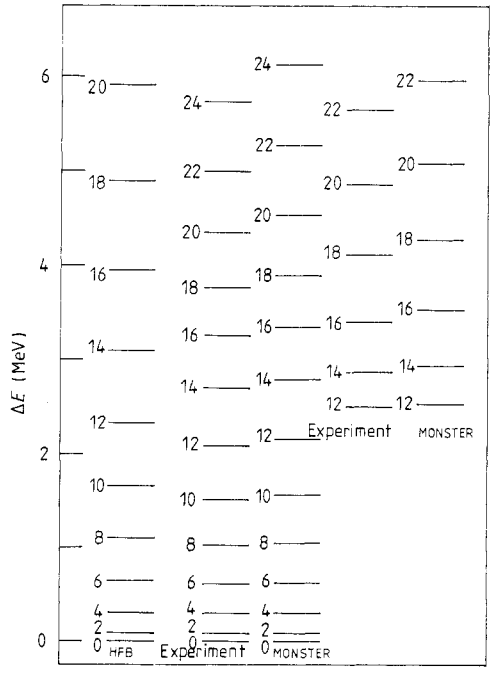

Figure 2. Ground and aligned bands in ^{164}Er: the MONSTER results are compared with the experimental data (Yates *et al* 1980). In addition the HFB spectrum is shown.

all, it is a typical transitional region of weakly deformed soft nuclei showing a shape change from deformed to spherical with decreasing proton number and increasing neutron number towards the $Z = 50$ and $N = 82$ magic cores, respectively. Since one expects the MONSTER to work best in strong and stable deformed nuclei, the performance of the model in such a case provides a crucial test for the underlying approximations. Secondly, recent experiments revealed a rich structure of sidebands in several nuclei around $A = 130$. Finally, a technical detail in favour of this region is that the single particle basis needed does not need to be as large as, for example, for rare earth nuclei.

In this investigation a single particle basis was chosen, which consists of the $N = 4$ major shell omitting the $0g_{9/2}$ state and including the negative parity levels $0h_{11/2}$, $0h_{9/2}$ and $1f_{7/2}$ for both protons and neutrons. The single particle energies were slightly modified with respect to the standard (Bohr and Mottelson 1969) values. As effective interaction a Brueckner G matrix was employed, which had been derived for nuclear matter starting with the Bonn one boson exchange potential (OBEP) as the bare nucleon-nucleon interaction (Holinde *et al* 1972). To be used for finite nuclei in a finite Hilbert space this force naturally had to be renormalised. This renormalisation was simulated here by a phenomenological procedure. Since it turned out that the original G matrix did not provide enough pairing correlations, attractive short-range terms of Gaussian shape were added with a range of $\mu = 0.5$ fm acting only in the $T = 1$ neutron-neutron and proton-proton channels. As strength parameters $V_{pp} = -120$ MeV and $V_{nn} = -50$ MeV were taken. This additional pairing force led to a decrease of the deformations, which was corrected by the introduction of an overall factor of 1.2 scaling all proton-neutron matrix elements.

That with this force the deformations in the whole mass region are reasonably well described can be seen from the $B(E2)$ values of the $2_1^+ \rightarrow 0_1^+$ transitions for several nuclei, which are shown in figure 3. The theoretical results have been calculated using fixed effective charges $e_p = (1+\chi)e$ and $e_n = \chi e$, with $\chi = 0.73$ being obtained by a least square fit to the Ce and Ba data. The theory describes quantitatively well the decreasing $B(E2)$ values towards the $N = 82$ and $Z = 50$ shell closures. For the $N = 66$ and $N = 70$ Xe isotopes the theory agrees better with the results from the earlier measurements (indexed by '1') (Kocher 1976). However, the high values from more reliable recent measurements (indexed by '2') (Hanewinkel *et al* 1983), where the estimated contributions of the side feeding were substracted, are an indication that the effective deformation of the Xe isotopes should be considerably larger than theoretically predicted. One obvious reason for this deficiency of the calculation could be the small number of valence protons (only four) for the Xe isotopes in the chosen model space. For a more consistent description of all nuclei in this mass region therefore a more balanced single particle basis containing also lower lying orbits at least for the protons should be used. On the other hand it would also be of great interest to perform careful revised experiments for the $B(E2)$ values of several other nuclei in this region in order to remove the impression of an uncertain experimental situation, which figure 3 definitely suggests.

Most sensitive to the spherical single particle energies, defining the one body term of the Hamiltonian, appeared to be the low lying spectra of the odd nuclei. Even the spin and parity of the ground state depend very sensitively on small shifts of the single particle levels close to the Fermi energy. Since one expects the lowest states in odd mass nuclei to be rather well described as a linear combination of projected one quasiparticle configurations, this approach was used to calculate the spectra of many

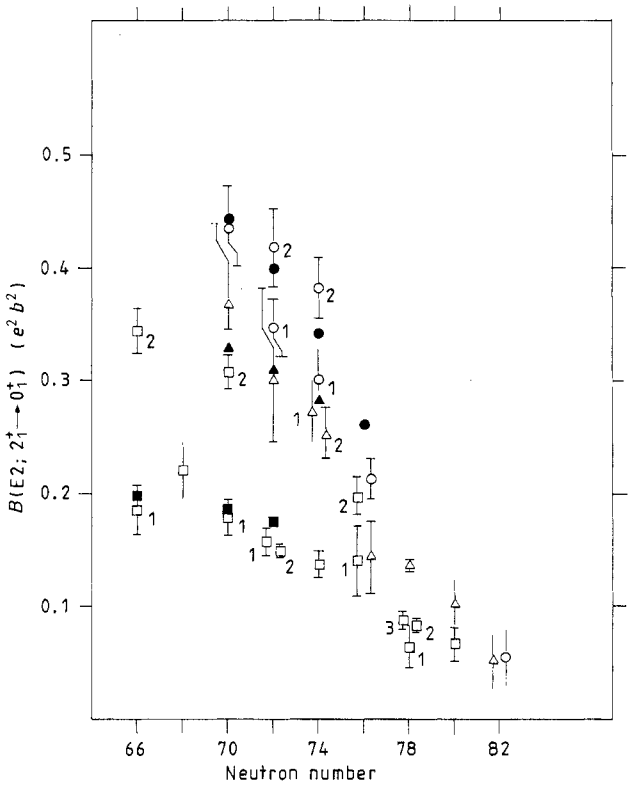

Figure 3. $B(E2)$ values in some $A = 130$ nuclei: the $B(E2)$ yrast transition probabilities to the ground state for some Ce (○), Ba (△) and Xe (□) isotopes are shown. The data taken from different experiments (for a complete list of references see Hammaren *et al* (1986a)) are indicated by open symbols and the theoretical results by the corresponding full symbols. $e_p = 1.73$, $e_n = 0.73$.

odd-even nuclei in the considered mass region. The spherical single particle energies have essentially been adjusted to the odd nuclei surrounding ^{130}Ba. Figure 4 shows a partial level scheme for the nucleus ^{129}Ba. Several experimentally known bands are compared with their theoretical counterparts (or at least candidates for them). The band heads are very well reproduced with the exception of the negative parity band, where the theoretically predicted $\frac{7}{2}$-band head is not seen in the experiment. Also the qualitative structure of the different bands is well reproduced, although for example the too small moment of inertia of the $\nu g_{7/2}$ band as well as the existence of several not yet well assigned low lying states seen experimentally indicate the need of also including three quasiparticle excitations in the theoretical description. Further information for a more or less unique deduction of the single particle energies can be obtained from the spectroscopic amplitudes for one particle transfer reactions. The distribution and fragmentation of the transfer strength allows us to draw more precise conclusions about the detailed position of single particle states also further away from the Fermi energy. For example the position of the $\nu d_{5/2}$ subshell was adjusted so that the experimental $l = 2$ strength distribution between 300 keV and 550 keV in ^{129}Ba was roughly reproduced, as can be seen in figure 5. Due to the restriction to one quasiparticle configurations only the theoretical strength is obviously more concentrated than the

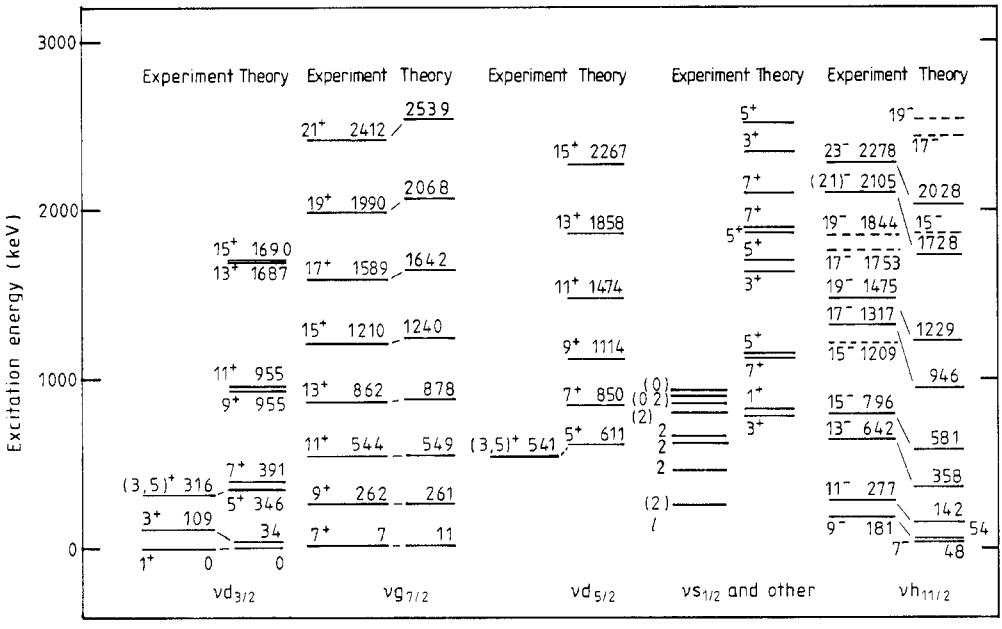

Figure 4. A partial level scheme of ^{129}Ba: several experimentally known bands (Griffioen and Sheline 1974) in ^{129}Ba are compared to the theoretical results obtained within the projected one quasiparticle approach.

more fragmented distribution seen in experiment. The theoretically predicted $l = 4$ $\nu g_{7/2}$ strength at only 7 keV above the ground state is not seen experimentally, but this may be understood because in the (d, t) reaction the strength for higher l values is strongly suppressed, and thus the small $l = 4$ distribution cannot be resolved from the much stronger $l = 0$ peak in this energy region. More refined experiments, which are able to measure the higher l distributions too, would be very helpful for a better determination of the single particle energies and also could provide first clues about the properties of the residual nucleon-nucleon interaction.

Having fixed the single particle energies and the 'renormalised' effective interaction as described above, a large number of nuclei in the $A = 130$ region were calculated without changing the Hamiltonian any more. In this way it was ensured that not just some selected data would be reproduced more or less by chance, and furthermore made it possible to test the quality of the Hamiltonian as well as the predictive power of the nuclear structure description. A comprehensive summary of the results of this systematic analysis of more than 50 nuclei in the $A = 130$ region was given by Hammaren *et al* (1985, 1986a, b). Here we want to show only some examples of these results. In figure 6 the energies and the intra-band $B(E2)$ values for the yrast bands of the isotopes ^{128}Ce up to ^{134}Ce are shown. In the upper row of the figure the excitation energies are plotted as functions of the total angular momentum. In the middle the transition energies $\Delta E(I \to I-2)$ are presented, which show the backbending effect in a much more pronounced form. In the lowest row finally the ratio of the $B(E2; I \to I-2)$ values and the corresponding values for a rigid rotor are displayed. The yrast band in ^{130}Ce had been used to determine the renormalisation parameters of the effective interaction. This explains the exceptionally good agreement with the experimental data in this particular case. All the other results shown have not been adjusted to the

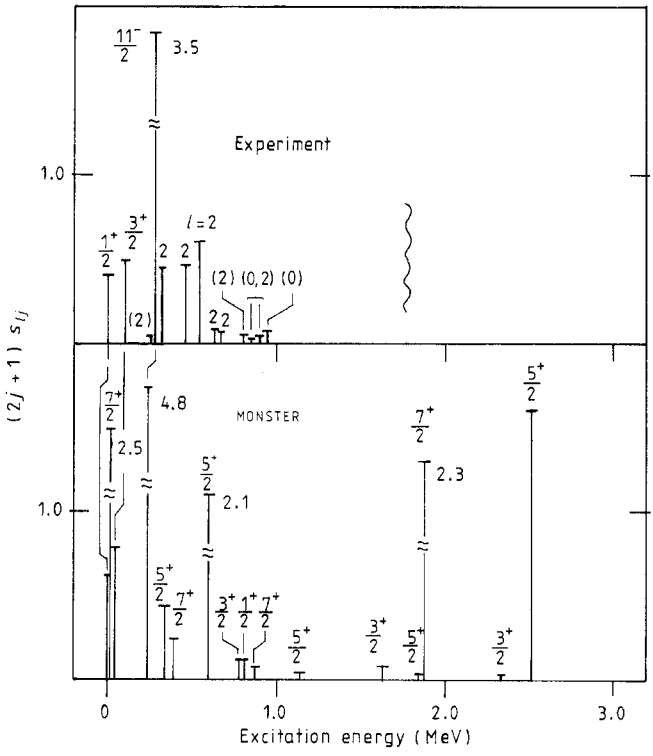

Figure 5. Spectroscopic amplitudes for one neutron pickup on ^{130}Ba: the theoretical amplitudes are compared with the experimental results obtained in a (d, t) reaction (Griffioen and Sheline 1974).

experimental data in any way. Regarding this fact surprisingly many features observable in these nuclei are well described. The moments of inertia at low angular momenta are reproduced without the necessity of introducing an effective core contribution, and their mass dependence is correctly described, too. The non-rotational behaviour of the γ ray energies within the yrast bands is nearly quantitatively reproduced, including the value of the critical angular momentum, which deviates from the observed values by at most 2 units. Up to ^{132}Ce the model predicts, in agreement with experimental arguments, that the $h_{11/2}$ protons form the crossing two quasiparticle band giving rise to the backbending behaviour. In ^{134}Ce, however, the lowest 10^+ state is calculated to have a distinct $h_{11/2}$ neutron origin in agreement with the g-factor measurement by Goldberg *et al* (1980). The calculated band is dominantly based on a projected $K = 10$ two quasiparticle configuration and shows practically no $B(E2)$ transitions to states with lower angular momenta than 10. Therefore we may call this band a K isomer with an effective K value $K_{\text{eff}} = 10$ (note that where the total wavefunction is a mixture of components with different K values K is not a good quantum number). The structure of the second 10^+ state, a $(\nu h_{9/2}, \nu h_{11/2})$ configuration, can be followed up to spin 14. Above spin 16 the yrast state turns out to be dominantly of a $(\pi h_{11/2})^2$ structure.

To complete the discussion of the Ce isotopes we show in figure 7 the calculated g factors for the considered Ce nuclei together with the experimental data for the 10^+ states in ^{134}Ce. The calculated g factors clearly demonstrate the nature of the ground

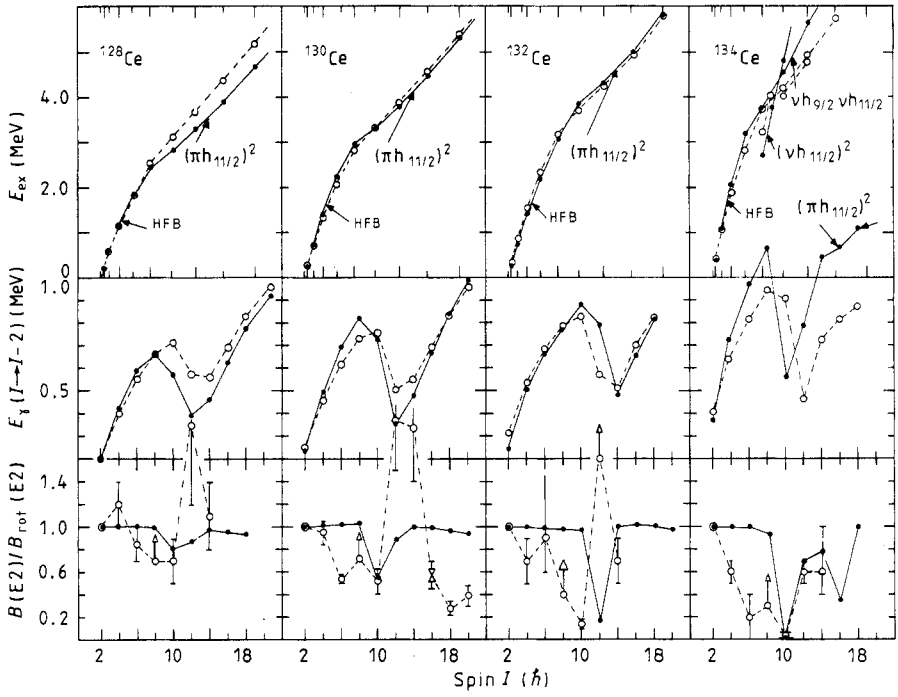

Figure 6. Yrast properties of some Ce isotopes: the excitation energies of the yrast states, the transition energies and the B(E2) transition probabilities normalised to the rotational values are all plotted as functions of the total angular momentum. The experimental data are indicated by open symbols connected by broken lines (for the compilation of the data see Hammaren *et al* (1986a)), whereas the results of the theory are shown with full circles connected by full lines.

and aligned bands in the Ce isotopes (see also §4.4). Up to the band crossing the values are slightly reduced from the simple collective estimate $g \sim Z/A \sim 0.4$. At the band crossing and beyond, the states with predominant proton character have large positive g factors, whereas the $(\nu h_{11/2})^2 K_{\text{eff}} = 10^+$ band in ^{134}Ce has a large negative value in good agreement with the experiment. The slight reduction of the g factor of the 10^+ state of the $\nu h_{9/2}\nu h_{11/2}$ band can nearly account for the observed negative g factor of the second 10^+ state, too.

Finally, as an example that the MONSTER approach cannot only be used to study the yrast bands and their properties, figures 8 and 9 present results for positive and negative parity excitations respectively in ^{128}Ba. Figure 8 summarises the results for the positive parity excitations in this nucleus. For each angular momentum the calculation yields typically about 100 excitations within 10 MeV above the yrast band. From these only the lowest ones are displayed in the figure. Using the calculated B(E2) transition probabilities some of these excitations have been grouped into bands. In this case the dominating two quasiparticle structure is indicated. As in the Ce isotopes, the model reproduces the ground band as well as the crossing aligned band rather nicely. It fails, however, to describe the second crossing band seen experimentally. In figure 9 the two experimentally known negative parity bands are compared with several candidates resulting from the calculation. The assignment of the experimental 7^- band as a $\nu g_{7/2}\nu h_{11/2}$ structure seems to be rather unambiguous, although

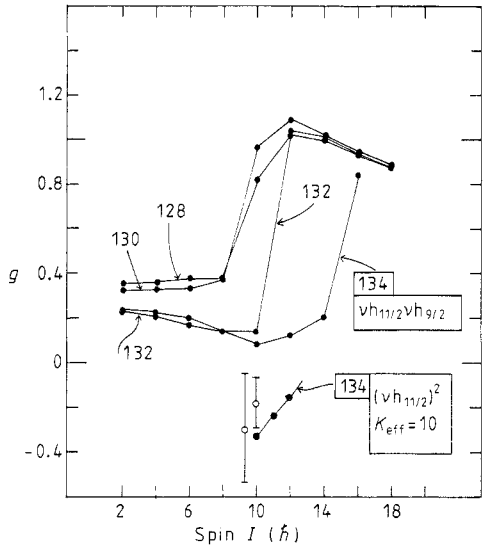

Figure 7. g factors of yrast excitations in Ce isotopes: the theoretical values (full circles connected by full lines) are calculated with the free values of the proton ($g_s^\pi = 5.587$, $g_l^\pi = 1.0$) and neutron ($g_s^\nu = -3.826$, $g_l^\nu = 0.0$) gyromagnetic factors. The upper set of calculated values for ^{134}Ce correspond to the members of the ground and the neutron ($h_{9/2}h_{11/2}$) bands and the lower set to the three lowest members of the neutron $(h_{11/2})^2 K = 10^+$ band. The experimental g factor with the smaller error bars is measured for the 10_1^+ state at 3208.4 keV (Goldberg *et al* 1980) and the one with the larger error bars for the 10_2^+ state at 3719.3 keV (Zemel *et al* 1982) in ^{134}Ce.

the energy of the band head is not so well reproduced. For the other experimental band there are several theoretical candidates and further information would be needed to allow for a clear interpretation.

3.3. Achievements and drawbacks

Summarising the discussion of the last section we may conclude that the MONSTER(HFB) approach is indeed a rather powerful tool for nuclear structure studies all over the mass table. The model is not restricted to the yrast properties of nuclei only but also yields a large number of non-yrast excitations accounting for collective as well as single particle like structures. It has been demonstrated that in small model spaces the method provides a rather satisfactory approximation to the complete SCM description. However, unlike the latter approach the MONSTER can be used also in rather large basis systems using general two body interactions, and thus allows for the first time microscopic, shell model like nuclear structure studies not only in light but also in medium heavy and heavy systems. The model produces 'clean' quantum mechanical many body wavefunctions with the proper symmetries and can hence not only be used to calculate expectation values like energies and moments but also to investigate any type of transition operators between the various excitations.

However, one should not forget that the MONSTER(HFB) approach uses a fixed mean field and severely truncated configuration spaces. Thus it accounts for only a limited number of degrees of freedom. Already for the description of doubly even nuclei this leads to a couple of limitations.

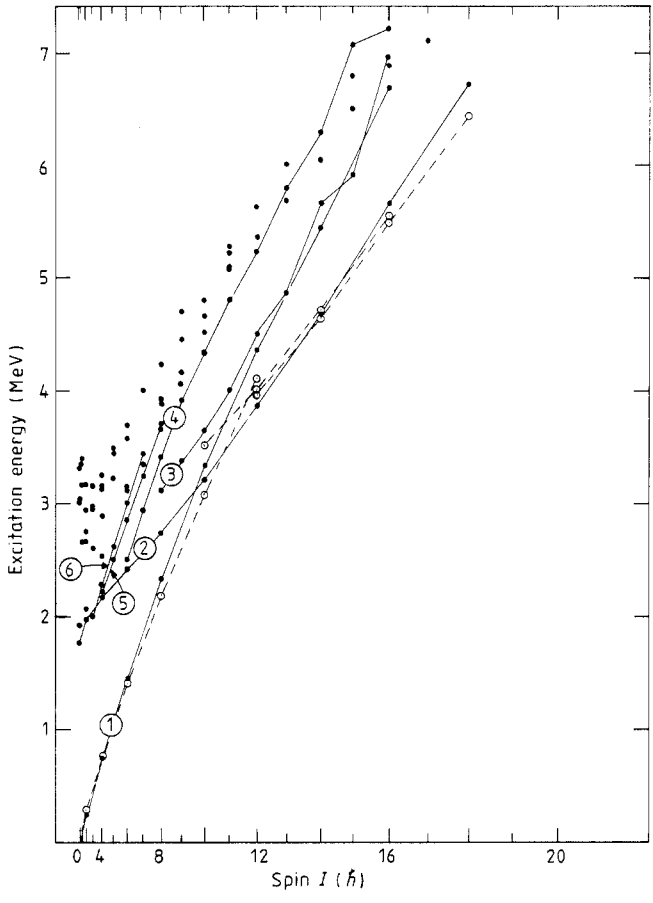

Figure 8. Positive parity bands in ^{128}Ba: experimental data (Schiffer *et al* 1983) for the ground and two excited positive parity bands (---○---) are presented together with the results of the MONSTER approach (—●—) for the lowest excitations. In the case where the theoretical results have been grouped into bands, the dominant two quasiparticle structure is indicated. 1, HFB + $(\nu h_{11/2})^2$, $K_{\text{eff}} = 0$; 2, $(\nu h_{11/2})^2$, $K_{\text{eff}} = 0$; 3, $(\nu h_{11/2})^2$, $K_{\text{eff}} = 8$; 4, $\nu d_{5/2}\nu g_{7/2}$, $K_{\text{eff}} = 6$; 5, $\nu d_{3/2}\nu g_{7/2}$, $K_{\text{eff}} = 4$; 6, $\nu d_{3/2}\nu g_{7/2}$, $K_{\text{eff}} = 3$.

(1) All dynamical changes in the structure of the wavefunctions with increasing spin or excitation energy have to be accounted for entirely by the configuration mixing of the included two quasiparticle configurations. It is obvious that with such a configuration space drastic changes of the structure of the nucleus like, for example, a change of its shape cannot be described properly.

(2) For the same reason the model becomes inadequate for the description of, for example, a second backbend in the yrast sequence, which implies the breakup of a further nucleon pair and hence a dominant four quasiparticle structure with respect to the fixed intrinsic vacuum. Thus there exists a natural limitation in angular momentum even for the description of the yrast band.

(3) Closely connceted to these deficiencies is also a deteriorating quality of the description of the non-yrast states with increasing angular momentum. While at low spin these excitations are still dominated by two quasiparticle structures, already at

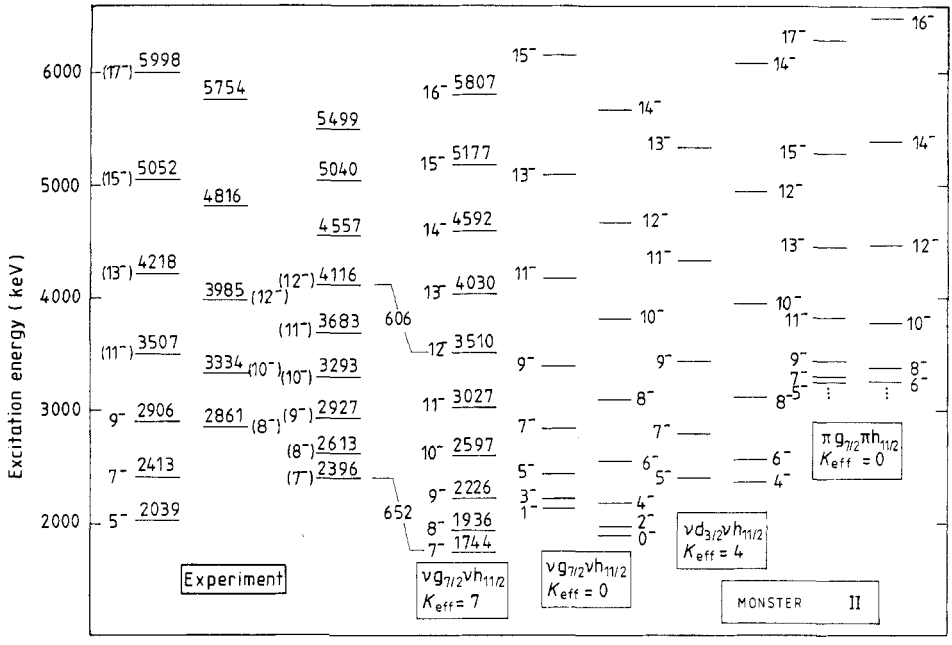

Figure 9. Negative parity bands in ^{128}Ba. Two experimental bands (Schiffer *et al* 1983) are compared with the four lowest negative parity bands resulting from the MONSTER approach.

the first backbend four quasiparticle configurations are expected to become rather important, which are not included in the configuration space.

For odd mass nuclei the MONSTER(HFB) approach performs even worse. Here, because of the restriction to projected one quasiparticle configurations, only band heads and low excited states can be expected to be described satisfactorily. In order to describe collective high spin phenomena with the same quality as in doubly even nuclei, here the three quasiparticle excitations would have to be included. The use of one quasiparticle excitations with respect to the fixed mean field of a doubly even nucleus leads to a further problem in the description of odd mass systems. The HFB vacuum used may be either the one of the neighbouring $(A+1)$- or $(A-1)$-doubly even nuclei. The results of the configuration mixing will depend on that choice, an ambiguity, which becomes serious especially near shell closures, where the mean field properties change rapidly with the mass number. Exactly the same problems are encountered in the description of odd-odd systems, where in addition to the one quasiproton-one quasineutron excitations in (3.3) now the one quasiproton-three quasineutron and three quasiproton-one quasineutron configurations would be needed in order to reach the same quality of the description in doubly even nuclei.

Obviously one could try to cure these deficiences by an extension of the configuration spaces. However, the inclusion, for example, the four quasiparticle excitations for even-even nuclei leads, at least in large model spaces, to practically unmanageable dimensions, and one is facing the same problems as the SCM method. Furthermore the extension of the configuration spaces would not solve the above discussed difficulties principally, but only shift them to a higher level. So, for example, if the four quasiparticle excitations were included for even-even nuclei, the same problem discussed above

for the second backbend would now occur at a possible third band crossing, and in a similar way also the other drawbacks would remain.

On the other hand, many of these shortcomings can be overcome in a rather natural way, if the concept of a fixed mean field for all states of a considered nucleus is given up. As a first step in this direction we shall show in the next section how the MONSTER(HFB) description can be improved by using optimised mean fields for each angular momentum separately.

4. Spin dependent mean fields: the MONSTER(VAMPIR) approach

In order to obtain the optimal mean field for a particular angular momentum (and given particle numbers), the HFB variational procedure described in § 3.1 has to be generalised. Considering an even mass system, instead of the symmetry breaking quasiparticle vacuum $|F\rangle$ (2.8), now a spin- and number-projected vacuum of the form (2.15) has to be used as test wavefunction. First attempts to formulate the variational equations for this HFB problem with projection before the variation go back as far as 1965 (Zeh 1965, 1967); however, until recently only strongly approximated solutions of this problem has been possible. In 1984 the problem was reformulated using the general mathematical tools outlined in § 2 of the present article (Schmid *et al* 1984a) and only shortly afterwards (Schmid *et al* 1984c, 1985) numerical solutions of the corresponding variational equations in basis systems of realistic size were presented. This method to obtain an optimal mean field for each spin separately was called the VAMPIR approach (variation after mean field projection in realistic model spaces).

Obviously the resulting mean fields can again be used to construct quasiparticle configuration spaces similar to those described in the previous chapter. If, for example, for an even mass system again only the projected two quasiparticle configurations on top of the projected vacuum are to be included, we obtain the MONSTER(VAMPIR) approximation, which differs from the MONSTER(HFB) approach by the use of different mean fields for different spin values instead of a fixed mean field for all angular momenta.

4.1. The variational equations

According to (2.15) the most general lab-frame wavefunction to be obtained from the HFB vacuum (2.8) has the form

$$|F_M^{NZI};a\rangle = \sum_{K=-I}^{+I} \boldsymbol{P}(NZIM;K)|F\rangle f_{Ka}^{NZI} \equiv \sum_K |F_{MK}^{NZI}\rangle f_{Ka}^{NZI} \tag{4.1}$$

where the mixing coefficients f had to be introduced in order to ensure that (4.1) is independent of the particular choice of the quantisation axis in the intrinsic frame of reference. $a=1,\ldots,m$ enumerates the different linear independent states obtained from the same intrinsic vacuum according to their energy. Because of the non-orthogonality of the $|F_{MK}^{NZI}\rangle$ with respect to K, in general m is not always equal to $2I+1$ but may be smaller.

The energy functional for the test wavefunction (4.1) is given by

$$E_{a=1}^{NZI}[F,f] = \frac{\langle F_M^{NZI};1|\boldsymbol{H}|F_M^{NZI};1\rangle}{\langle F_M^{NZI};1|F_M^{NZI};1\rangle} \tag{4.2}$$

and depends (at least for $I \neq 0$) not only on the HFB transformation F but also on the mixing coefficients f. Variation of (4.2) with respect to f^{NZI*}_{K1} yields the matrix equation

$$\sum_{K'} [\langle F^{NZI}_{MK}|\boldsymbol{H}|F^{NZI}_{MK'}\rangle - E^{NZI}_1 \langle F^{NZI}_{MK}|F^{NZI}_{MK'}\rangle] f^{NZI}_{K'1} = 0 \tag{4.3}$$

which like (3.5) represents the diagonalisation of a Hermitian matrix in a non-orthogonal basis. The orthonormality of the m linear independent solutions of (4.3) is ensured by the constraint

$$\sum_{KK'} f^{NZI*}_{Ka} \langle F^{NZI}_{MK}|F^{NZI}_{MK'}\rangle f^{NZI}_{K'b} = \delta_{ab} \qquad a, b = 1, \ldots, m \tag{4.4}$$

which closely resembles (3.6).

The variation with respect to the HFB transformation is more complicated. F is a $(2M \times 2M)$ matrix. However, because of its special form (2.5) and its unitarity only $M(M-1)/2$ linear independent combinations of its elements do exist. A useful method to construct these linear independent variables explicitly is provided by Thouless' theorem (Thouless 1960). The essence of this theorem is that starting from an arbitrary HFB vacuum $|F_0\rangle$ of the form (2.8) any other vacuum $|F_d\rangle$ being non-orthogonal to $|F_0\rangle$ can be represented as

$$|F_d\rangle = c(d) \exp(\tfrac{1}{2} \sum_{\mu\nu} d_{\mu\nu} a^+_\mu(F_0) a^+_\nu(F_0))|F_0\rangle \tag{4.5}$$

with

$$c(d) \equiv \langle F_0|F_d\rangle \tag{4.6}$$

and d being an antisymmetric $(M \times M)$ matrix. The quasiparticle operators belonging to the new vacuum $|F_d\rangle$ are related to those of the reference vacuum $|F_0\rangle$ by

$$\begin{pmatrix} a^+ & (F_d) \\ a & (F_d) \end{pmatrix} = F_d \begin{pmatrix} c^+ \\ c \end{pmatrix} = G_d \begin{pmatrix} a^+ & (F_0) \\ a & (F_0) \end{pmatrix} \tag{4.7}$$

where

$$G_d \equiv F_d F_0^+ = \begin{pmatrix} L_d^{-1*} & -(L_d^{-1} d)^* \\ -L_d^{-1} d & L_d^{-1} \end{pmatrix} = (G_d^+)^{-1} \tag{4.8}$$

is again a unitary $(2M \times 2M)$ transformation. The matrix L_d ensures the orthonormality of the new quasiparticle orbits. It is of lower triangular form and can be uniquely determined by a Cholesky decomposition (see, e.g., Wilkinson 1965) of the $(M \times M)$ matrix

$$1 + d^{\mathrm{T}} d^* \equiv L_d L_d^+. \tag{4.9}$$

Equations (4.5)-(4.9) give a unique parametrisation of the transformation F_d in terms of $M(M-1)/2$ independent variables. Thus the variation of (4.2) with respect to F can be replaced by a variation with respect to the matrix elements $d_{\alpha\beta}$ $(\alpha < \beta = 1, \ldots, M)$. This method has also been widely used in conventional intrinsic HFB and self-consistent cranking calculations (see, e.g., Ring and Schuck 1980).

Variation of the energy functional (4.2) with respect to the $d_{\alpha\beta}$ yields a set of equations for the global gradient vector

$$g_{\alpha\beta} \equiv (L_d^{-1\mathrm{T}} \tilde{g}_d L_d^{-1})_{\alpha\beta} = 0 \qquad \alpha < \beta = 1, \ldots, M \tag{4.10}$$

where the local gradient $\tilde{g}_d$ is defined by an antisymmetric $(M \times M)$ matrix

$$(\tilde{g}_d)_{\gamma\delta} \equiv \sum_{KK'} f^{NZI*}_{K1} \langle F_d|(\boldsymbol{H} - E^{NZI}_1 \mathbf{1}) \boldsymbol{P}(NZIK; K') a^+_\gamma(F_d) a^+_\delta(F_d)|F_d\rangle f^{NZI}_{K'1}. \tag{4.11}$$

From (4.11) it becomes obvious that the VAMPIR wavefunction (4.1) resulting from the simultaneous solution of the above equations does not mix via the Hamiltonian with any projected two quasiparticle configuration based on the same mean field. This is a sort of generalised Brillouin theorem for the VAMPIR states (4.1).

The system of equations (4.3), (4.4) and (4.10) is not yet sufficient to determine the transformation F_d unambiguously. This is due to the fact that the vacuum $|F_d\rangle$ is invariant under any unitary transformation of the quasiparticle annihilators $a(F_d)$. This so-called third Bloch-Messiah transformation (the matrix C in (2.7)) can be used to diagonalise any Hermitian $(M \times M)$ matrix. In the VAMPIR approach for this purpose as in conventional intrinsic HFB theory the H^{11} part of the Hamiltonian in the quasiparticle representation F_d is taken (see, e.g., Schmid *et al* 1984a).

Let us assume that for a particular spin value and given particle numbers the above equations have been solved and the corresponding HFB transformation $F(NZI)$ has been obtained. Using this transformation instead of the fixed mean field for the construction of the configuration spaces (3.3) and (3.4) we obtain the MONSTER(VAMPIR) approach, which differs from the MONSTER(HFB) approximation only by the fact that different mean fields are used for different angular momenta.

It should be pointed out that in the MONSTER(VAMPIR) approach because of (4.10) the VAMPIR solution (4.1) and the projected two quasiparticle excitations based on the same mean field are energetically demixed. The yrast state for each spin value is therefore described here entirely by a single projected zero quasiparticle determinant. Because of the non-orthogonality of the projected vacuum with respect to the projected two quasiparticle configurations, however, the non-yrast states with the same angular momentum cannot be described by linear combinations of the latter alone but have to be properly orthogonalised with respect to (4.1). This can be done either explicitly or, mathematically equivalent, by adding the various K components of (4.1) to the many particle basis as is done in (3.3). In the latter case (3.6) takes care of the orthonormality.

4.2. Numerical solution

Mathematically the solution of the VAMPIR variational equations is equivalent to the minimisation of a function of many variables. Thus one way to attack this problem would be the use of a gradient method, which has been successfully applied, for example, in the self-consistent cranking approach (Mang *et al* 1976, Egido *et al* 1980). In this method always a step in the direction of the local gradient (4.11) would be used to update the wavefunction, the resulting $|F_d\rangle$ then serving as new reference vacuum $|F_0\rangle$. The procedure would then be repeated until $|F_0\rangle$ and $|F_d\rangle$ coincide. However, this method is numerically not very stable, especially if the function to be minimised depends strongly only on some variables, while the dependence on others is very weak. A detailed discussion of the deficiencies of the gradient method in such cases has been given by Kowalik and Osborne (1968). In order to avoid these numerical instabilities usually a rather small step size in the gradient direction has to be chosen and consequently a lot of iterations are needed before convergence is achieved. This may be a minor problem for simple functions; for the VAMPIR approach, however, in which both the calculation of the energy functional as well as the local gradient vector are rather time consuming, it becomes a serious if not unbridgeable obstacle. Therefore we adopted (Schmid *et al* 1984c) another strategy, the so-called BFGS method (Brodlie 1977). In order to apply this quasi Newton method to our problem we have to keep

the reference frame $|F_0\rangle$ fixed and to work with the global gradient vector (4.10). The procedure can be summarised as follows.

(1) One defines a search direction w^i for the ith iteration by the product of an approximate inverse Hessian matrix H^{i-1} with the gradient vector (4.10) at the current variable vector d^i

$$w^i = -H^{i-1} g^i. \tag{4.12}$$

This is based on the idea that a step in this direction would lead to the exact minimum of a quadratic form if $(H^{i-1})^{-1}$ were the corresponding exact matrix of the second derivatives. Initially, for H^0 an appropriately scaled positive definite diagonal matrix is chosen.

(2) One now looks for a minimum of the energy E_1^{NZI} (to be determined as the energetically lowest solution of (4.3) and (4.4)) in the direction w^i defined by (4.12), i.e. one minimises the function

$$f(\alpha) = E_1^{NZI}(d^i + \alpha w^i) \tag{4.13}$$

with respect to α. The resulting α^i is then used to calculate an updated variable vector

$$d^{i+1} = d^i + \alpha^i w^i. \tag{4.14}$$

In practice this linear search can be performed approximately, requiring only an appropriate decrease of the function value as well as of the directional derivative in the search direction.

(3) The inverse Hessian matrix is now updated using the information about the change of the gradient vector

$$y^i = g^{i+1} - g^i \tag{4.15}$$

via the BFGS formula

$$H^i = H^{i-1} + \frac{1}{w^{iT} y^i}\left[\left(1 + \frac{y^{iT} H^{i-1} y^i}{w^{iT} y^i}\right) w^i w^{iT} - H^{i-1} y^i w^{iT} - w^i (H^{i-1} y^i)^T\right]. \tag{4.16}$$

Steps 1 to 3 are now repeated until the norm of the gradient vector (4.10) is smaller than a given convergence limit. At the convergence point $(H^i)^{-1}$ becomes the matrix of the second derivatives of the functional (4.2), i.e. the stability matrix of the VAMPIR approach.

This numerical method has been the essential key to the numerical feasibility of the VAMPIR approach in realistic calculations. Tests with simple polynomials in a few variables show that using the BFGS procedure about two orders of magnitude in the number of function (and gradient) evaluations can be gained with respect to the gradient method, if the latter converges at all. In practical applications (see § 4.4) usually only 20 to 40 iterations were needed to achieve convergence.

4.3. Approximations

In order to make applications of the VAMPIR and MONSTER(VAMPIR) approaches in large basis systems numerically feasible, up to now the same symmetry restrictions on the HFB transformation had to be imposed, which were already used for the MONSTER(HFB) approximation.

(1) The mixing of proton with neutron states in the transformation (2.5) is neglected. Therefore the intrinsic VAMPIR vacua $|F(NZI)\rangle$ contain only pairing correlations between like nucleons. Furthermore, this approximation restricts the application of the VAMPIR approach to doubly even nuclei.

(2) Parity mixing via the transformation (2.5) is not allowed. Consequently $|F(NZI)\rangle$ has positive parity.

(3) Finally, axial symmetry is enforced on the quasiparticle transformation. Thus $|F(NZI)\rangle$ has total angular momentum projection $K = 0$ and is time-reversal invariant. As a consequence $|F(NZI)\rangle$ contains only components with even spin values.

Using these approximations the variable matrix d can be written as

$$d_{\alpha\beta} = \delta_{\pi_\alpha \pi_\beta} \delta_{\tau_\alpha \tau_\beta} \delta_{-m_\alpha m_\beta} d_{\alpha\bar{\beta}} \tag{4.17}$$

where $\bar{\beta}$ denotes the time-reversed partner of the quasiparticle state β. Thus, using the antisymmetry of d and its time-reversal properties, there are for example only 18 independent variables of the type (4.17) within a (1s0d) basis, while for a (0s0p1s0d1p0f2s1d0g) basis 230 and for the Kumar-Baranger basis ($N = 4, 5$ for protons and $N = 5, 6$ for neutrons) 231 such variables do exist. Such systems can still be handled rather easily with the VAMPIR approach.

Note, that because of (4.17) the Brillouin theorem (4.10) now does hold only for projected two quasiparticle configurations with $K = 0$. Thus, in MONSTER(VAMPIR) calculations using the above approximations the VAMPIR yrast states with $I > 0$ may still be lowered by the dynamical admixture of those projected two quasiparticle configurations in the basis (3.3) which have $K \neq 0$. Further implications of the above approximations will be discussed in § 4.5.

4.4. Examples for applications

As a first example for a realistic application of the VAMPIR approach we shall discuss here some calculations for the yrast bands in ^{130}Ce and ^{128}Ba (Schmid *et al* 1985) using exactly the same single particle basis and Hamiltonian as in the systematic study of the $A = 130$ mass region (Hammaren *et al* 1985, 1986a, b) with the MONSTER(HFB) approach, results of which have already been presented in the previous section. In this basis the number of independent variables (4.17) is 96. Figure 10 presents the yrast spectra of ^{130}Ce as obtained by spin and number projection after the variation from the intrinsic HFB vacuum, by the conventional MONSTER(HFB) approach based on this intrinsic vacuum and by the above discussed VAMPIR approach, and compares them with the experimental data. As can be seen, both the MONSTER(HFB) calculation, including about 130 two quasiparticle configurations, as well as the VAMPIR approach, yielding only one projected determinant for each spin value, reproduce the experimental data rather nicely. The backbending is predicted at the right spin value, and for the moments of inertia of both the ground as well as of the aligned band the agreement is very satisfactory, too. As the insert shows, this holds even if differential quantities like the transition energies are compared. A careful analysis of the absolute energies, however, reveals that the VAMPIR solutions for the 0^+, 2^+, 4^+ and 14^+ to 20^+ states are about 50 to 500 keV stronger bound than the MONSTER(HFB) yrast states. For the other spin values (6^+ to 12^+) the MONSTER(HFB) results are a few to 50 keV lower, thus indicating some contribution from projected $K \neq 0$ two quasiparticle configurations in this spin region. Obviously here an improvement of the VAMPIR yrast states in the MONSTER(VAMPIR) approach is to be expected.

Figure 11 shows the corresponding results for ^{128}Ba. Again rather good agreement with the experimental data is obtained, though here the MONSTER(HFB) approach produces the backbending two spin units too early as compared to the VAMPIR and experimental results.

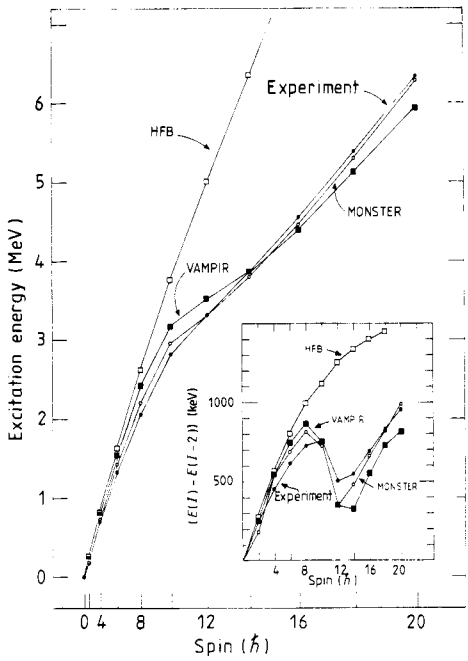

Figure 10. Yrast band in ^{130}Ce: the excitation energy is plotted against the total spin in $I(I+1)$ scale. The full circles refer to the experimental data (Todd *et al* 1984), open circles to the MONSTER(HFB) approach. Projection from the corresponding intrinsic vacuum alone yields the open squares. Full squares, finally, refer to the VAMPIR approach. The insert shows the corresponding backbending plots, i.e. the spin dependence of the transition energy $E(I)-E(I-2)$, which can be interpreted as being about twice the rotational frequency at this spin value.

The VAMPIR calculations for ^{130}Ce and ^{128}Ba revealed two different mechanisms causing the backbending in these two nuclei. The former nucleus has only about two protons in the $h_{11/2}$ shell. Hence in the rotating frame of reference the Coriolis force is strong and thus, as expected from the simple phenomenological description of Stephens and Simon (1972), the well known alignment of a quasiparticle pair in a high-spin orbit results. In ^{128}Ba, on the other hand, the $h_{11/2}$ proton orbit is almost empty. As already indicated by the MONSTER(HFB) calculations, here the backbending is produced by the $h_{11/2}$ neutrons, in spite of the fact that in the ground state this orbit is slightly more than half filled and hence the Coriolis interaction is small. However, the nucleus helps itself by first scattering a neutron pair from the $h_{11/2}$ level into energetically nearby empty $g_{7/2}$ neutron states and thus increasing the available alignment energy. This effect was predicted some years ago (Grümmer *et al* 1979).

These two different mechanisms causing the backbend are demonstrated in figures 12-15. Figures 12 and 13 display the occupations of the different spherical basis states as functions of the total angular momentum in the two considered nuclei, respectively. As can be seen from figure 12 in ^{130}Ce first with increasing spin a slight rearrangement of the neutrons in the $h_{11/2}$ and $g_{7/2}$ orbits is observed, while the occupations of all other protons and neutron orbits stay almost constant. At the backbend the neutron $h_{11/2}$ and $g_{7/2}$ occupations nearly recover their ground-state values, while the $h_{11/2}$ proton occupation suddenly increases from about 1.3 to 2 particles. Thus here the full alignment energy of a $h_{11/2}$ pair becomes available. Except for the much

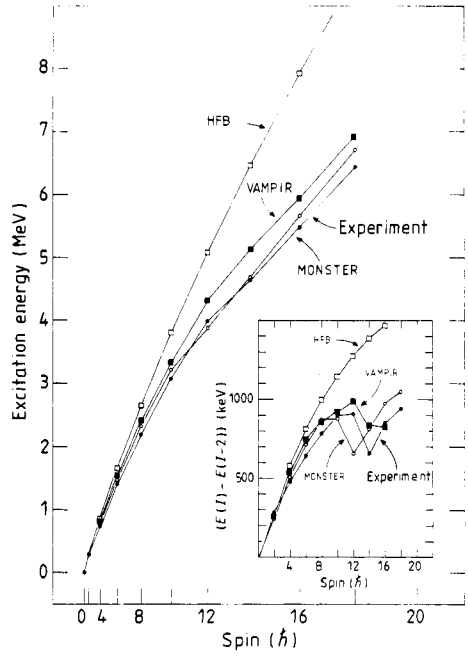

Figure 11. Yrast band in ^{128}Ba: the same conventions as in figure 10 are used. The experimental data are here from Schiffer *et al* (1983).

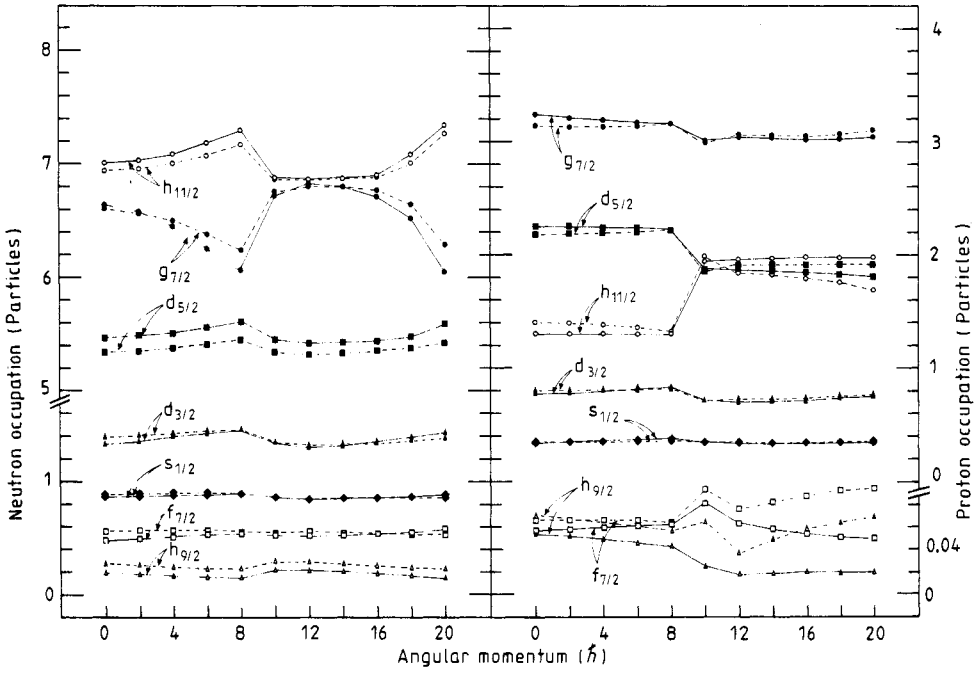

Figure 12. Occupation of single particle states in ^{130}Ce: the neutron occupations are given on the left ($N_v = 22$), the proton ones on the right ($Z_v = 8$) side of the figure. Broken lines connect the results from the intrinsic, full ones those obtained from the spin and number projected VAMPIR vacua.

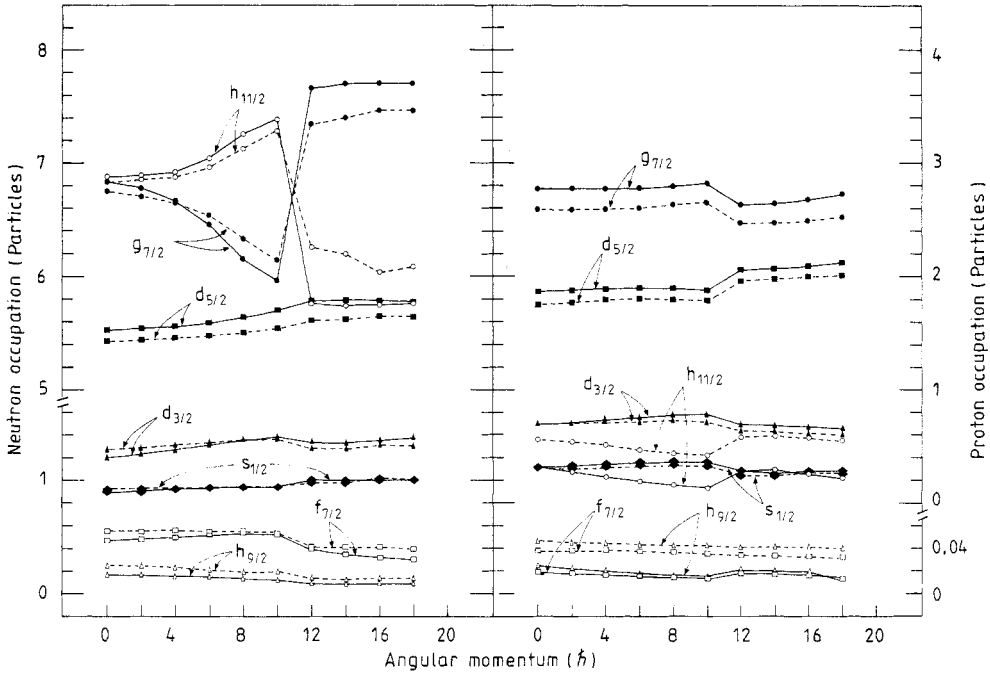

Figure 13. Occupation of single particle states in ^{128}Ba: the same conventions as in figure 12 are used.

smaller $h_{11/2}$ proton occupation, before the backbend the occupation numbers of ^{128}Ba (figure 13) show almost the same properties as those of ^{130}Ce. At the backbend, however, the situation becomes different. Here the above mentioned sudden decrease of the $h_{11/2}$ neutron occupation in ^{128}Ba by almost two particles accompanied by an equally drastic increase of the $g_{7/2}$ neutron occupation is observed. In other words a neutron pair is scattered from the $h_{11/2}$ into the $g_{7/2}$ orbit.

It can be seen that in ^{130}Ce the $h_{11/2}$ protons and in ^{128}Ba the $h_{11/2}$ neutrons are really causing the backbend by decomposing the total angular momentum of each VAMPIR yrast state into its individual contributions from the particles in the different spherical basis orbits (Schmid *et al* 1986a). For this purpose we write the total angular momentum operator as

$$\boldsymbol{I}_\mu \equiv \boldsymbol{J}_\mu(\tau nlj) + \boldsymbol{R}_\mu(\tau nlj) \qquad \mu = -1, 0, 1 \tag{4.18}$$

where

$$\boldsymbol{J}_\mu(\tau nlj) \equiv \left(\frac{j(j+1)(2j+1)}{3}\right)^{1/2} (c^+_{\tau nlj} c_{\tau nlj})^1_\mu \tag{4.19}$$

is the angular momentum operator for the spherical basis orbit τnlj with

$$(c^+_{\tau nlj} c_{\tau nlj})^1_\mu \equiv \sum_{mm'} (-1)^{j-m'} (jj1|m-m'mu) c^+_{\tau nljm} c_{\tau nljm'} \tag{4.20}$$

and

$$\boldsymbol{R}_\mu(\tau nlj) \equiv \sum_{\tau' n' l' j' \neq \tau nlj} \left(\frac{j'(j'+1)(2j'+1)}{3}\right)^{1/2} (c^+_{\tau' n' l' j'} c_{\tau' n' l' j'})^1_\mu \tag{4.21}$$

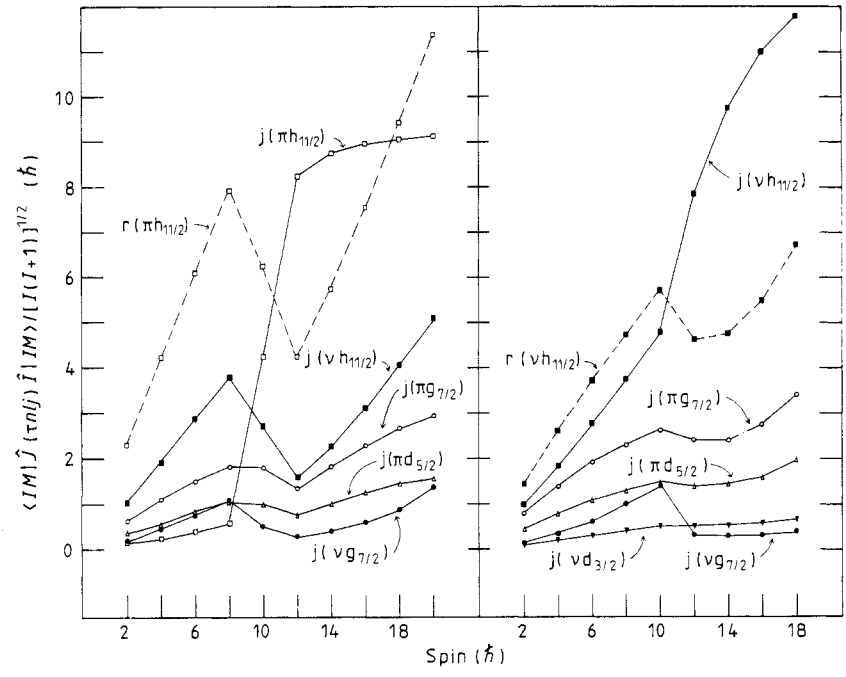

Figure 14. Decomposition of the total angular mometum for ^{130}Ce and ^{128}Ba: the individual contributions from the nucleons in different sphereical basis orbits (4.23) to the total angular momentum are presented as functions of the total spin. For ^{130}Ce furthermore the total contribution of all orbits excluding the $h_{11/2}$ proton level, for ^{128}Ba the total contribution excluding the $h_{11/2}$ neutron level (4.24), are displayed.

contains the contributions of all other orbits. Calculating the spectroscopic amplitudes

$$S_I^{\tau nlj} \equiv \langle F^{NZI} \| (c^+_{\tau nlj} c_{\tau nlj})^1 \| F^{NZI} \rangle \tag{4.22}$$

within the VAMPIR wavefunctions (4.1) and using simple angular momentum algebra (Edmonds 1957), we obtain the angular momentum contribution of the particles in a certain spherical basis state τnlj in the direction of the total angular momentum $\boldsymbol{I}$ as

$$J(\tau nlj) \equiv \frac{\langle IM|\boldsymbol{J}(\tau nlj)\boldsymbol{I}|IM\rangle}{[I(I+1)]^{1/2}} = \frac{\langle F^{NZI} \| \boldsymbol{J}(\tau nlj) \| F^{NZI} \rangle}{(2I+1)^{1/2}} \tag{4.23}$$

as well as the contribution of all other orbits in this direction

$$R(\tau nlj) = [I(I+1)]^{1/2} - J(\tau nlj). \tag{4.24}$$

Figure 14 displays the 'alignments' (4.23) of the particles in some spherical orbits as functions of the total angular momentum $\boldsymbol{I}$ for the yrast states of both considered nuclei. It is clearly seen that in ^{130}Ce the backbending is caused by the two $h_{11/2}$ protons, which contribute almost nothing to the total angular momentum up to spin $\boldsymbol{I} = 8$ and then suddenly at $\boldsymbol{I} = 10$ become the dominant component. Simultaneously the contributions of all other orbits with the $h_{11/2}$ neutrons being the dominant component show a decrease in the backbending region as can be seen from the 'collective' angular momentum $R(\pi h_{11/2})$. In ^{128}Ba, having the same neutron number as ^{130}Ce, at low spins the $h_{11/2}$ neutrons again dominate the rotation. However, because of the missing $h_{11/2}$ protons here the $h_{11/2}$ neutrons themselves do align and cause the backbending effect.

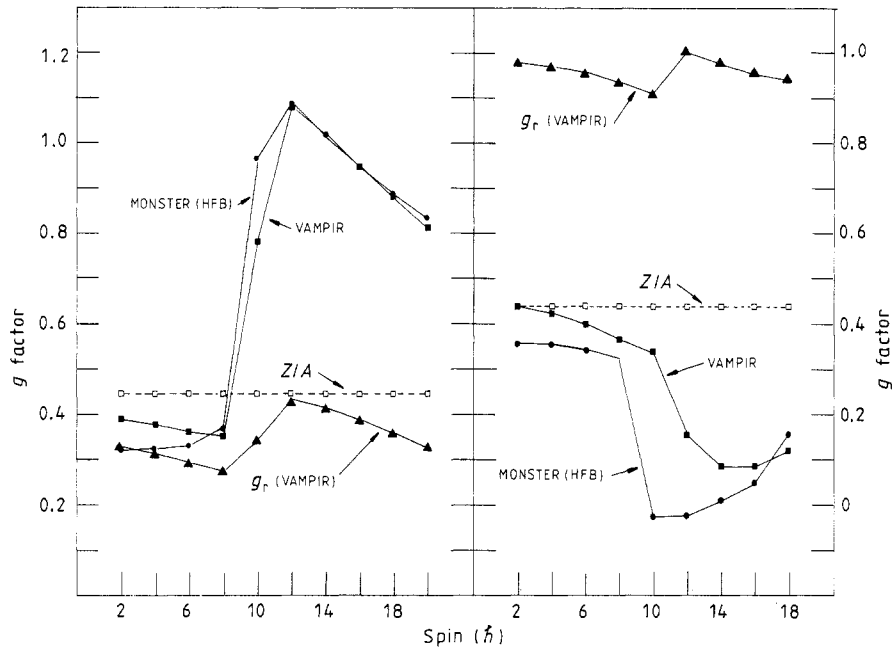

Figure 15. g factors for ^{130}Ce and ^{128}Ba: the results of the MONSTER(HFB) and the VAMPIR approach for the yrast bands are compared with each other and with the expected collective model g factor Z/A. Furthermore the collective g factors g_R(VAMPIR) are presented, which have been obtained with the help of the alignments displayed in figure 14 via (4.25).

Closely connected to these alignments are the g factors displayed in figure 15. In fact, with the g factor of a free proton being positive and that of a neutron being negative, the change of this quantity at the backbend gives rather direct information as to whether this effect is caused by a proton or a neutron alignment. In the first case a sudden increase of the g factor (as obtained for ^{130}Ce), in the latter one a sudden decrease (as seen for ^{128}Ba) would be expected. The total g factors can be furthermore decomposed into a 'collective' contribution g_R and a 'valence' contribution $g(\tau nlj)$

$$g^I = g_R^I + \frac{g^I(\tau nlj) - g_R^I}{[I(I+1)]^{1/2}} J(\tau nlj) \tag{4.25}$$

with $J(\tau nlj)$ given by (4.23). Using the g^I calculated with the VAMPIR approach (the MONSTER(HFB) results are very similar and will hence not be discussed here separately), the alignments from figure 14 and free values for the valence g factors ($g(\pi h_{11/2}) = 1.417$ for ^{130}Ce, $g(\nu h_{11/2}) = -0.348$ for ^{128}Ba) one obtains from (4.25) the collective g factors labelled by g_R(VAMPIR) in figure 15. The latter vary indeed only smoothly with the angular momentum. In ^{130}Ce, furthermore, the g_R(VAMPIR) has almost the usual Z/A value, so that here in the total g factor really a single particle effect on top of the collective rotation is observed. In ^{128}Ba, on the other side, the g_R(VAMPIR) is a good factor of 2 larger than Z/A and thus indicates that most of the $h_{11/2}$ neutrons participate mainly in the collective rotation.

Up to now in this section only applications of the VAMPIR approach alone, i.e. for yrast bands, have been discussed. As an example for a full MONSTER(VAMPIR) calculation we present therefore in figure 16 the spectrum of ^{22}Ne as obtained in a (1s0d)

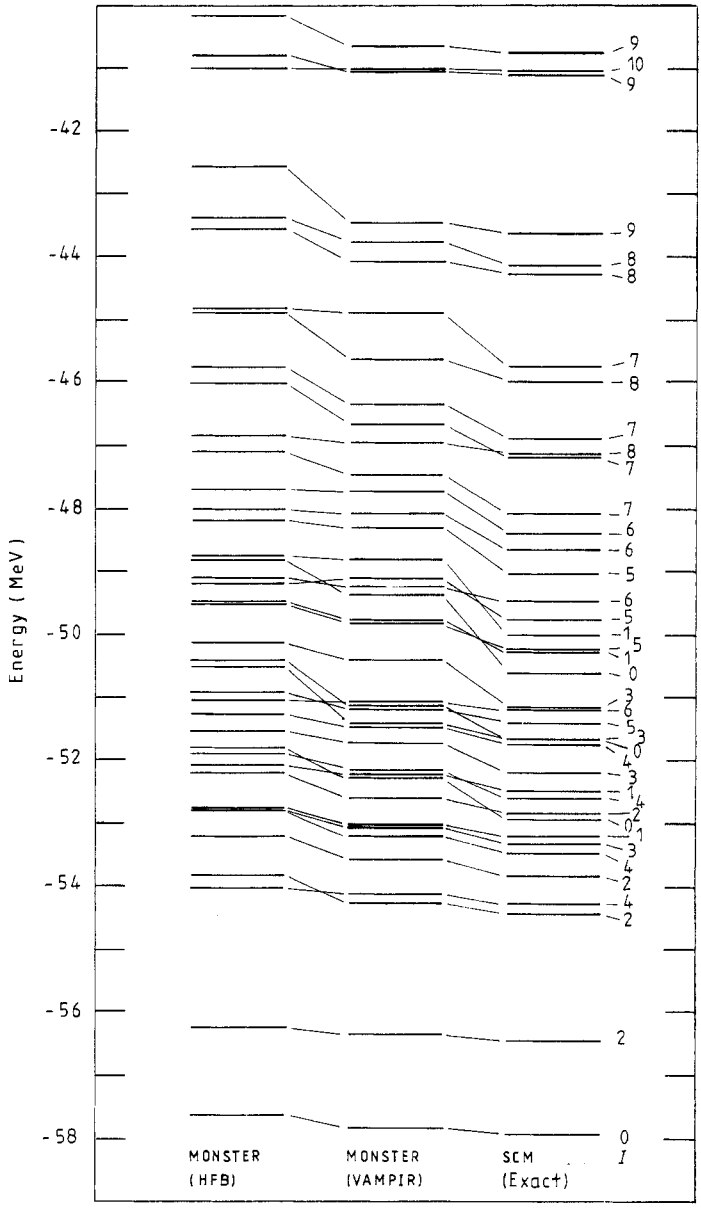

Figure 16. Spectrum of ^{22}Ne obtained in a (1s0d)-basis: the results of a conventional MONSTER(HFB) calculation are compared with those resulting from the MONSTER(VAMPIR) approach and with the exact SCM solutions.

basis using the same Hamiltonian as for figure 1. In this application (Schmid *et al* 1984c) the rather small basis was taken in order to make a comparison of the MONSTER(HFB) and MONSTER(VAMPIR) results with those of an exact SCM diagonalisation possible. In figure 16 for each spin value (except for $I = 9$ and 10) the four lowest states obtained with these three different methods have always been included. As can be seen, in this particular case the MONSTER(HFB) approach always yields a fair

agreement with the exact results, but the MONSTER(VAMPIR) calculation does even better. Here the yrast states as well as many non-yrast levels (altogether about half of the levels displayed) agree within 250 keV with the exact solutions. For the other half of the states the agreement is not so perfect, the worst case being the fourth 0^+ and 1^+ states, both being more than 1 MeV off. The reason for this (though still very moderate) disagreement is partly due to the approximations discussed in § 4.3, partly caused by principal limitations of the MONSTER(VAMPIR) approach. Both aspects will be discussed in the following section.

It should be pointed out here that the agreement between the MONSTER(HFB) and MONSTER(VAMPIR) approaches is not always as good as in the particular case of ^{22}Ne. This becomes rather obvious for doubly magic nuclei like ^{16}O or ^{40}Ca. There intrinsic HFB calculations yield a spherical mean field without pairing correlations and consequently the MONSTER(HFB) approach reduces then to a kind of one particle-one hole approximation. The VAMPIR approach, on the other hand, due to the spin and number projections before the variation yields in general a pair-correlated deformed mean field even in doubly magic nuclei and a corresponding ground-state energy considerably (a few MeV) lower than the one obtained in the MONSTER(HFB) approximation. An example for this superiority of the MONSTER(VAMPIR) approach especially near shell closures will be discussed in § 5.

4.5. Achievements and drawbacks

Compared with the MONSTER(HFB) approximation the MONSTER(VAMPIR) approach has a couple of considerable advantages. First of all, since the VAMPIR procedure optimises the mean field for each spin separately, even drastic changes of the intrinsic structure with increasing spin (like for example shape transitions, etc) become microscopically describable. Furthermore, for the same reason, the model works principally up to arbitrary high angular momentum equally well, though a natural technical limitation is obviously induced by the size of the chosen single particle basis. In addition, since the number projections are also performed before the variation, the model performs much better in the neighbourhood of shell closures where the nuclear properties change very rapidly with the mass number. Last but not least, since the two quasiparticle configurations in (3.3) are now always constructed with respect to the optimal mean field for the corresponding yrast state, the quality of the description of the excited non-yrast states does not deteriorate any more with increasing angular momentum as was the case in the MONSTER(HFB) approximation.

Nevertheless, in spite of these achievements, the model still has a couple of shortcomings, which may be classified into two different types. The first type is caused by the approximations discussed in § 4.3 and may hence be subsumed under the term 'technical deficiencies'.

(1) Since parity mixing the HFB transformation is neglected, the VAMPIR approach produces optimal mean fields only for positive parity states. Obviously via the configuration mixing in the MONSTER(VAMPIR) approach the negative parity states come in. However, there is some ambiguity as to which of the various mean fields obtained for the positive parity states should be used for the construction of the configuration space (3.3) for the negative parity levels of a particular angular momentum. Of course one can try all of them and take that one which produces the energetically lowest negative parity yrast state for this spin value, however, this is not the 'optimal' mean field for this problem. Technically this deficiency could be overcome by allowing parity mixing

in the quasiparticle transformation (2.5) and using parity projected configurations of the type (2.18) in the calculation. Simple estimates show that such a scheme could only be incorporated in the model without causing too many additional numerical difficulties.

(2) However, even if parity mixing were allowed, because of the restriction to axial symmetric transformations, the VAMPIR could still produce optimal mean fields only for the natural parity states. For the unnatural parity excitations again one has to rely on the configuration mixing (3.3) and hence introduces the same ambiguity as discussed above. Releasing the axial symmetry of (2.5), however, yields two additional numerical integrations for the angular momentum projection and is hence far more complicated than the inclusion of parity mixing. Nevertheless, with the present speed of improvement of the computer facilities, even the use of non-axial transformations in the model may become feasible.

(3) Even with parity and axial symmetry being broken, because of the neglect of proton-neutron mixing in the HFB transformation, optimal mean fields could still only be obtained for doubly even nuclei and hence the description of, e.g., odd-odd systems via the configuration mixing (3.3) will still display the same shortcomings as discussed in § 3. In order to obtain optimal mean fields also for odd-odd systems proton-neutron mixing in the transformation (2.5) should be allowed.

Even if all the above discussed technical drawbacks could be overcome there will still remain a second type of shortcoming of more fundamental nature and will therefore be referred to as 'principal deficiencies' in the following.

(1) The prescription to use the mean field obtained via the VAMPIR approach for the yrast state of a given spin also for the construction of the projected two quasiparticle configurations does not in general lead to the deepest energy minimum in the configuration space (3.3) with the transformation F being left free. This is due to the fact that in the MONSTER(VAMPIR) approach first the mean field is obtained by a variational procedure for a single projected determinant and then the configuration mixing is performed with the mean field being fixed. To obtain the deepest minimum, however, the coupling of these two types of degrees of freedom should be accounted for by performing both variations simultaneously. This leads to the MAD (many determinant) VAMPIR approach, which was already formulated a couple of years ago (Schmid *et al* 1984a) and will be discussed in § 6.

(2) For odd nuclei, because of the even number parity of the HFB vacuum $|F\rangle$, the same problems as discussed in the context of the MONSTER(HFB) approximation remain. Especially here the MAD VAMPIR would yield a considerable improvement.

(3) Finally, the most severe drawback of the MONSTER(VAMPIR) approach is due to the fact that the mean field is always optimised for the yrast state of a given spin value and in addition only the projected two quasiparticle configurations based on this yrast mean field are included. Consequently, the MONSTER(VAMPIR) approach yields a rather good description for the yrast bands as well as for those excited non-yrast states, which have a similar intrinsic structure as the corresponding yrast configuration. However, there are many other states in the nuclear spectrum (e.g. shape isomers, many particle-many hole structures, etc), which are rather different from the corresponding yrast state and hence not accessible within the truncation scheme of the MONSTER(VAMPIR) approach. In order to describe also such states the concept of a single mean field for all states of a given angular momentum has to be given up, and instead different mean fields for different excited states have to be introduced. How this can be done will be described in the next section.

5. Self-consistent description of non-yrast states: the EXCITED VAMPIR approach

The idea of obtaining optimised mean fields for each state of a given spin separately by a chain of variational calculations for projected determinants, with the current test wavefunction always being constrained to be orthogonal to all the solutions already calculated, has already been elaborated by us some years ago (Schmid and Grümmer 1979) for the case of spin projected HF configurations. Later it was extended to the more general case of projected HFB type determinants (Schmid *et al* 1984a). However, at that time numerical solutions of the corresponding variational equations still seemed almost impossible. Furthermore, it turned out later on that the original idea of ensuring the orthogonality with the help of Lagrangian multipliers for the projected overlaps between the current test wavefunction and the solutions already obtained, which was guided by similar calculations in the intrinsic frame of reference (see, e.g., Mang *et al* 1976), could not be used for general projected determinants. This is due to the fact that the projection operator (2.16) admixes to any intrinsic configuration almost all other quasiparticle determinants constructable in the chosen model space. Therefore it is extremely difficult, and in some cases even impossible, to obtain vanishing projected overlaps between two arbitrary quasiparticle configurations. The breakthrough came when the problem was reformulated by incorporating the orthogonality constraint explicitly. This was done in the EXCITED VAMPIR approach (Schmid *et al* 1986b), which will be discussed in this section.

5.1. Theory

Let us assume that we have obtained the VAMPIR solution $|F_M^{NZI}; 1\rangle$ (4.1) for the yrast state of a certain nucleus and a particular angular momentum. Suppressing the obvious spin and number quantum numbers for convenience, we may write this state in shorthand notation as

$$|\Psi^1\rangle \equiv |\Phi^1\rangle\beta_1^1 \equiv |F_M^{NZI}; 1\rangle \tag{5.1}$$

with

$$|\Phi^1\rangle \equiv \sum_K \boldsymbol{P}(NZIM; K)|F^1\rangle f_{K1}^1 \tag{5.2}$$

and the upper index '1' indicating that the yrast solution is meant. For the first excited state with the same spin we then use the test wavefunction

$$|\Psi^2\rangle \equiv |\Phi^1\rangle\beta_1^2 + |\Phi^2\rangle\beta_2^2 \tag{5.3}$$

with

$$|\Phi^2\rangle \equiv \sum_K \boldsymbol{P}(NZIM; K)|F^2\rangle f_{K1}^2 \tag{5.4}$$

having the same form as (5.2) and the coefficients β_1^2 and β_2^2 to be determined by requiring normalisation and orthogonality with respect to the yrast state (5.1). One obtains easily that

$$\beta_2^2 = \langle\Phi^2|(1 - |\Phi^1\rangle\langle\Phi^1|\Phi^1\rangle^{-1}\langle\Phi^1|)|\Phi^2\rangle^{-1/2} \tag{5.5}$$

and

$$\beta_1^2 = -\langle\Phi^1|\Phi^1\rangle^{-1}\langle\Phi^1|\Phi^2\rangle\beta_2^2. \tag{5.6}$$

Variation of the energy functional for (5.3) with respect to the HFB transformation F^2 and the mixing coefficients f^2 then yields a solution for the first excited state, which is obviously orthogonal to the yrast solution (5.1).

This procedure (being equivalent to a Gram-Schmidt orthogonalisation) can be easily generalised for the case of more than two states. Let us assume that by successive variation we have already obtained $n-1$ orthonormal solutions of the form

$$|\Psi^i\rangle = \sum_{j=1}^{i} |\Phi^j\rangle \beta_j^i \qquad i = 1, \ldots, n-1 \tag{5.7}$$

with $|\Phi_j\rangle$ always being of the form (5.2)

$$|\Phi^j\rangle = \sum_K \boldsymbol{P}(NZIM; K)|F^j\rangle f_{K1}^j \tag{5.8}$$

and

$$\langle\Psi^i|\Psi^j\rangle = \delta_{ij} \qquad i, j = 1, \ldots, n-1. \tag{5.9}$$

For the nth test wavefunction we then make the ansatz

$$|\Psi^n\rangle = \sum_{j=1}^{n-1} |\Phi^j\rangle \beta_j^n + |\Phi^n\rangle \beta_n^n \tag{5.10}$$

where

$$|\Phi^n\rangle = \sum_K \boldsymbol{P}(NZIM; K)|F^n\rangle f_{K1}^n \equiv \sum_K |\chi_K\rangle f_{K1}^n. \tag{5.11}$$

By requiring $|\Psi^n\rangle$ to be normalised and orthogonal to all the $|\Psi^i\rangle$ $(i = 1, \ldots, n-1)$ already obtained one derives

$$\beta_n^n = \langle\Phi^n|\left(1 - \sum_{j,l=1}^{n-1} |\Phi^j\rangle (A^{-1})_{jl} \langle\Phi^l|\right)|\Phi^n\rangle^{-1/2} \tag{5.12}$$

with A^{-1} being the inverse of the overlap matrix

$$A_{jl} \equiv \langle\Phi^j|\Phi^l\rangle \qquad i, j = 1, \ldots, n-1 \tag{5.13}$$

and

$$\beta_j^n = -\sum_{l=1}^{n-1} (A^{-1})_{jl} \langle\Phi^l|\Phi^n\rangle \beta_n^n. \tag{5.14}$$

Defining the projection operator

$$\boldsymbol{S} \equiv \sum_{j,l=1}^{n-1} |\Phi^j\rangle (A^{-1})_{jl} \langle\Phi^l| \tag{5.15}$$

it is a straightforward exercise to show that the energy functional for the test wavefunction (5.10) has the form

$$E_1^n \equiv \langle\Psi^n|\boldsymbol{H}|\Psi^n\rangle = \frac{\langle\Phi^n|(1-\boldsymbol{S})\boldsymbol{H}(1-\boldsymbol{S})|\Phi^n\rangle}{\langle\Phi^n|(1-\boldsymbol{S})|\Phi^n\rangle} \tag{5.16}$$

which corresponds to the total variational space spanned by (5.11) with $n-1$ linear independent solutions of this form being projected out.

Variation of (5.16) with respect to $(f^n_{K'1})^*$ then yields again a matrix equation of the type (4.3)

$$\sum_{K'}(H_{KK'}-E^n_1 N_{KK'})f^n_{K'1}=0 \tag{5.17}$$

being constrained by

$$f^{n*}Nf^n=1 \tag{5.18}$$

being the unit matrix. Here we have used the definitions

$$N_{KK'}\equiv\langle\chi_K|(1-\boldsymbol{S})|\chi_{K'}\rangle \tag{5.19}$$

and

$$H_{KK'}\equiv\langle\chi_K|(1-\boldsymbol{S})\boldsymbol{H}(1-\boldsymbol{S})|\chi_{K'}\rangle \tag{5.20}$$

for the overlap and Hamiltonian matrices N and H, respectively. $|\chi_K\rangle$ is given by (5.11). For the variation with respect to F^n we again use the parametrisation (4.5) via the Thouless theorem

$$|F^n_d\rangle=c(d)\exp\left(\tfrac{1}{2}\sum_{\mu\nu}d_{\mu\nu}a^+_\mu(F^n_0)a^+_\nu(F^n_0)\right)|F^n_0\rangle \tag{5.21}$$

with respect to an arbitrary reference vacuum $|F^n_0\rangle$. Variation of (5.16) with respect to $d_{\alpha\beta}$ then yields again a sort of Brillouin theorem

$$\left(\sum_{\gamma\delta}(L^{-1}_d)_{\gamma\alpha}\sum_{KK'}f^{n*}_{K1}\langle F^n_d|(1-\boldsymbol{S})(\boldsymbol{H}-E^n_1)(1-\boldsymbol{S})\boldsymbol{P}(NZIK;K')\right.$$
$$\left.\times a^+_\gamma(F^n_d)a^+_\delta(F^n_d)|F^n_d\rangle f^n_{K'1}(L^{-1}_d)_{\delta\beta}\right)\langle\Phi^n|(1-\boldsymbol{S})|\Phi^n\rangle^{-1}=0 \tag{5.22}$$

for the configuration $|\Phi^n\rangle$. (5.22) is the straightforward generalisation of (4.10) for the case of restricted variational spaces.

Equation (5.17), (5.18) and (5.22) (together with an ovbious diagonalisation of H^{11} in the F^n_d representation in order to fix the third Bloch-Messiah transformation as discussed in § 4.1) are the variational equations of the EXCITED VAMPIR approach. Their solution creates successively a set of orthonormal A nucleon wavefunctions, (5.7) and (5.10), for a given spin value, each of them being based on a different mean field and being energetically stable against arbitrary projected two quasiparticle excitations with respect to the corresponding vacuum. Thus the residual interaction between these states is automatically minimised by the above procedure and hence the EXCITED VAMPIR dynamically provides an optimal basis for the A nucleon problem. Note that because of the appearance of the projector $\boldsymbol{S}$ in (5.16) the non-diagonal elements between the $|\Psi^i\rangle$ $(i=1,\ldots,n)$ are obtained as a byproduct of the solution. Thus after having obtained the n lowest solutions $|\Psi^i\rangle$ by the variational procedure the wavefunctions can be once more improved by diagonalising the residual interaction

$$\sum_{j=1}^{n}(\langle\Psi^i|\boldsymbol{H}|\Psi^j\rangle-E_\alpha\delta_{ij})g_{j\alpha}=0 \tag{5.23}$$

where

$$(g^+g)_{\alpha\beta}=\delta_{\alpha\beta}\qquad\alpha,\beta=1,\ldots,n. \tag{5.24}$$

The most general wavefunctions to be obtained from the EXCITED VAMPIR approach, therefore, have the form

$$|\varphi_\alpha\rangle \equiv \sum_{j=1}^{n} |\Psi^j\rangle g_{j\alpha} \tag{5.25}$$

and account even in the yrast state for additional correlations going beyond the VAMPIR approximation (4.1).

As far as the numerical solution is concerned, the similarity of the EXCITED VAMPIR equations (5.17), (5.18) and (5.22) with the corresponding VAMPIR variational equations (4.3), (4.4) and (4.10) makes it obvious that exactly the same method can be used as described in § 4.2. Because of the appearance of the projector $(1-\boldsymbol{S})$ in the above equations, however, the numerical effort in each of the n variational calculations increases linearly in i, with i being the actual number of the calculation. Thus in order to create n solutions $|\Psi^i\rangle$ roughly $n(n+1)/2$ times the computer time of a single VAMPIR calculation is needed. With n being 5 this gives a factor of 15, which is still bearable even in very large basis systems.

As far as additional approximations are concerned up to now exactly the same symmetry restrictions of the HFB transformation as discussed in § 4.3 have also been imposed onto the EXCITED VAMPIR approach. This leads obviously to the same 'technical deficiencies' as discussed in § 4.5. We shall come back to this point below.

5.2. Examples for applications

As an example of the application of the EXCITED VAMPIR approach we shall discuss here results for the four lowest $I^\pi = 0^+$ states in ^{50}Ti as obtained in a full (1p0f)-shell basis (Schmid *et al* 1986b). As effective two body interaction here the renormalised G matrix of Kuo and Brown (1968) with the modifications of the $(f_{7/2})^2$ matrix elements introduced by McGrory (1973) has been used. The single particle energies have also been taken from the latter work except that the $f_{7/2}$ level has been lowered by 0.5 MeV with respect to the other three orbits. Using this Hamiltonian then the $I^\pi = 0^+$ states have been calculated in the MONSTER(HFB), the MONSTER(VAMPIR) and the above described EXCITED VAMPIR approach with $n = 4$. The results are displayed in figure 17. The energy scale is defined by setting the lowest ground-state energy (obtained by diagonalising the residual interaction between the four lowest 0^+ solutions obtained with the EXCITED VAMPIR via (5.23) and (5.24)) to zero. As can be seen in this nucleus the MONSTER(HFB) approach fails completely. This is due to the fact that the intrinsic HFB mean field yields here a $(f_{7/2})^8$ shell closure on the neutron side and a spherical BCS type solution for the proton part of the wavefunction. Because of the $(\nu f_{7/2})^8$ configuration the neutron two quasiparticle excitations reduce here to one particle-one hole configurations. Since now the proton part of the HFB vacuum has spin zero, too, and none of the neutron one particle-one hole states can be coupled to angular momentum zero, the MONSTER(HFB) approach yields no 0^+ states resulting from neutron excitations. Consequently it can only produce four 0^+ states corresponding to a diagonalisation of the Hamiltonian in the $|(\nu f_{7/2})^8(\pi j)^2 0^+\rangle$ shell model configurations with j being any of the four orbits of the (1p0f) shell. These four 0^+ states are displayed in the leftmost column of figure 8. They have obviously nothing to do with the experimental data. This is one of the examples for the bad performance of the MONSTER(HFB) approach near shell closures discussed in the previous section. The MONSTER(VAMPIR) approach performs much better here. Because of the projection

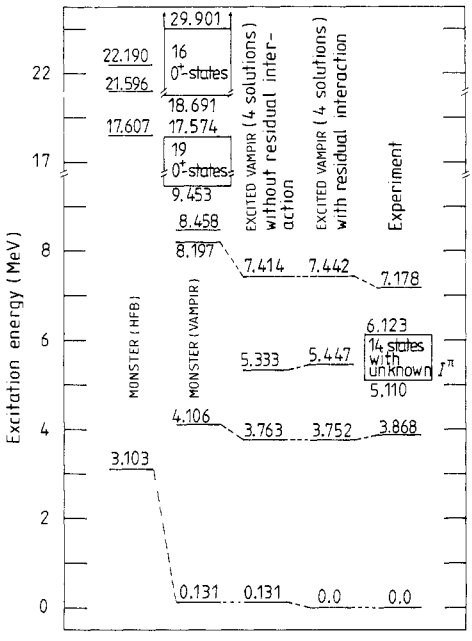

Figure 17. $I = 0$ states in ^{50}Ti: the results obtained for the four lowest 0^+ states obtained by the EXCITED VAMPIR model with and without the residual interaction are compared with those of the MONSTER(HFB) approach as well as with those of the MONSTER(VAMPIR) description and with the experimental data (taken from the compilation by Alberger (1984)).

before the variation the $(f_{7/2})^8$ neutron closure is broken as well as the spherical symmetry. Instead a 0^+ yrast state is obtained which is based on a slightly prolate deformed intrinsic vacuum containing pairing correlations in the neutron as well as in the proton part of the wavefunction. The corresponding energy is almost 3 MeV lower than the MONSTER(HFB) result. For the excited states the improvement is even more dramatic. Here now 38 linear independent 0^+ states as compared to the three of the MONSTER(HFB) calculation are obtained, the lowest one being more than 13 MeV more bound than the one of the latter approach. However, the EXCITED VAMPIR approach using only $n = 4$ different projected determinants still does much better. Even with the residual interaction not being diagonalised (in this case the yrast state is identical to the VAMPIR solution) the first excited 0^+ is lowered by 343 keV, the third excited one by 783 keV with respect to the corresponding MONSTER(VAMPIR) states. Furthermore as the second excited 0^+ a new state now appears, which was not obtained before. It turns out that this state is based on an oblate deformed intrinsic configuration, while the other three 0^+ levels result from prolate intrinsic determinants. This is an example that in the EXCITED VAMPIR approach even states with a completely different structure than the corresponding yrast state become easily accessible in a rather natural way. Diagonalisation of the residual interaction between these four solutions yields the second but last spectrum from the left. The effect of this diagonalisation is almost negligible and thus supports the statement that the EXCITED VAMPIR indeed minimises the residual interaction between its different solutions. Unfortunately in experiments no 0^+ state has been assigned in the energy region where the oblate solution is predicted. However, since there are 14 states with unknown I^π assignment observed in this region there is a fair chance that the predicted state may also be found experimentally.

In the meantime we have been able to perform EXCITED VAMPIR calculations in much larger model spaces. So for example the lowest five 0^+ states in ^{40}Ca have been studied in a full (0s0p1s0d1p0f2s1d0g)-shell basis using a realistic G matrix for the two body part and the matrix elements of the kinetic energy operator for the one body part of the Hamiltonian. The first results of this investigation are rather encouraging. So for example the lowest excited 0^+ at 3.35 MeV as well as the next 0^+ excitation seem to be reproduced rather nicely. Very promising results are also obtained for the lowest excited 0^+ states in ^{28}Si and ^{16}O. However, since these investigations are not yet published and their results may still undergo some quantitative changes by adjusting the G matrix to the chosen basis system we shall not comment on them any further in the present article.

5.3. Achievements and drawbacks

The main advantage of the EXCITED VAMPIR approach as compared to the MONSTER(VAMPIR) model results from the fact that the mean field is optimised for each state separately by a new variational calculation and not only adjusted to the yrast configuration. Thus, while the latter approach is restricted to the yrast states and small amplitude excitations with respect to them, in the EXCITED VAMPIR approach, at least in principle, excitations of arbitrary complexity can be described. Furthermore, by construction this approach minimises the residual interaction between its different solutions and hence successively creates an optimal many particle basis for the A nucleon problem at a given angular momentum. Thus already with a small number of configurations an excellent description of the nuclear properties can be reached. Last but not least by its chain of variational calculations the approach automatically determines the relevant degrees of freedom for each particular state under consideration irrespective of whether they are of collective or single particle nature. In this way one avoids the one-sidedness introduced by 'guessing' *a priori* some collective coordinates as it is done for example in the generator coordinate method (Hill and Wheeler 1953).

Indeed, except for the restriction to even A systems induced by the number parity of the HFB type intrinsic vacua being used in the test wavefunctions, the EXCITED VAMPIR approach has no 'principal' drawbacks. It should be applicable to any kind of arbitrary complex nuclear excitations (always provided that one can determine the appropriate effective Hamiltonian reasonably well). However, it has to be stressed that the 'technical deficiencies' of the VAMPIR approach induced by the symmetry restrictions on the HFB transformation, which have been discussed in § 4.5, obviously hold for the EXCITED VAMPIR approach in its present form, too. Thus at the moment the approach is limited to even spin positive parity states in doubly even nuclei and only after allowing for parity non-conservation, non-axiality and isospin mixing in the transformation (2.5) other states, as well as odd-odd nuclei, would become accessible.

Finally, one practical complication caused by the present approximations in both the VAMPIR as well as the EXCITED VAMPIR approach should be mentioned. Because of the axial symmetry in general a prolate reference vacuum $|F_0\rangle$ yields also a prolate solution $|F_d\rangle$, while an oblate reference induces an oblate solution. Thus in order to be on the safe side, each variational calculation has to be done with two different references having opposite deformations. This is somewhat tedious, but is the price one has to pay for the simplifications gained by this symmetry restriction.

6. A preview: the MAD VAMPIR description and beyond

Let us now turn our attention to the question of what could be done to still improve the scope of our theory besides breaking the remaining symmetries in the quasiparticle transformation. We have already discussed in § 4.5 that in general the MONSTER(VAMPIR) approach will not yield the deepest possible energy minimum in the configuration space (3.3), since the variations with respect to the mean field and configuration mixing degrees of freedom are not performed simultaneously but one after the other. Thus an obvious improvement of the MONSTER(VAMPIR) approach would be to use the full ansatz (3.7) as test wavefunction with both the configuration mixing coefficients f as well as the HFB transformation F as free variational parameters instead of taking F from a preceding VAMPIR calculation. However, the resulting variational equations for such a MAD (many determinant) VAMPIR description in the full two quasiparticle space are rather messy (Schmid *et al* 1984a) and, at least with the present computer facilities, probably numerically unsolvable. On the other hand the situation becomes different if instead of a large number of configurations as in (3.3) only relatively few span the considered configuration space. This is, for example, the case for odd-A systems where the configuration space (3.4) consisting of all one quasiparticle states with respect to a mean field still to be determined by a simultaneous variation together with the configuration mixing would obviously be a rather good approximation. Since such a description would overcome the only common 'principal' deficiency of all the above discussed approaches, namely their inability to cope with odd-A systems, we shall discuss this method in the present section, though its numerical feasibility has up to now only been estimated and not yet proven by a realistic calculation.

6.1. The basic equations

Let us consider a limited configuration space consisting of m projected quasiparticle determinants

$$\zeta(NZI) \equiv \{|Q^{NZI}_{MK}(F)\rangle \equiv \boldsymbol{P}(NZIM; K)|Q(F)\rangle;\ K = -I, \ldots, +I;\ Q = 1, \ldots, m\} \tag{6.1}$$

being all based on the same HFB transformation F with the $|Q(F)\rangle$ being, for example, all the one quasiparticle configurations. Then the most general test wavefunction has the form

$$|a;\ NZIM\rangle = \sum_{Q=1}^{m} \sum_{K=-I}^{+I} |Q^{NZI}_{MK}(F)\rangle f^{NZI}_{KQ;a} \tag{6.2}$$

with the label a enumerating the linear independent states according to their energy. Variation of the corresponding energy functional with respect to $f^{NZI*}_{KQ;a}$ then yields our standard matrix equations (3.5) and (3.6), where here the overlap and Hamiltonian matrices N and H are given by

$$N_{KQ;K'Q'} \equiv \langle Q^{NZI}_{MK}(F)|Q'^{NZI}_{MK'}(F)\rangle \tag{6.3}$$

and

$$H_{KQ;K'Q'} \equiv \langle Q^{NZI}_{MK}(F)|\boldsymbol{H}|Q'^{NZI}_{MK'}(F)\rangle \tag{6.4}$$

respectively. The variation with respect to the transformation F can again be performed using the Thouless parametrisation (see, e.g., (4.5)). Here one obtains

$$\sum_{KK'QQ'} f^{NZI*}_{KQ;1} f^{NZI}_{K'Q';1} \sum_{\gamma\delta} \{(L^{-1})_{\gamma\alpha} \langle Q(F)|(\boldsymbol{H}-E_1)\boldsymbol{P}(NZIK;K')a^+_\gamma(F)a^+_\delta(F)|Q'(F)\rangle (L^{-1})_{\delta\beta}$$

$$+(L^{-1})^*_{\gamma\alpha}\langle Q(F)|(\boldsymbol{H}-E_1)\boldsymbol{P}(NZIK;K')a_\gamma(F)a_\delta(F)|Q'(F)\rangle \tag{6.5}$$

$$\times (L^{-1})^*_{\delta\beta}\} = 0$$

where $\alpha < \beta = 1, \ldots, M$. In the case that all the $|Q(F)\rangle$ are one quasiparticle configurations the second term of (6.5) obviously vanishes. The same is true if (6.1) is restricted to the projected vacuum and an arbitrary number of two quasiparticle determinants only, or even more general, if with any intrinsic configuration $|Q(F)\rangle$ all determinants $a_\gamma(F)a_\delta(F)|Q(F)\rangle$ are either vanishing or again contained in the many particle basis. Then, because of (3.5), (6.5) again simplifies to a sort of Brillouin theorem, namely

$$\sum_{\gamma\delta}(L^{-1})_{\gamma\alpha} \sum_{KK'QQ'} f^{NZI*}_{KQ;1}\langle Q(F)|(\boldsymbol{H}-E_1)\boldsymbol{P}(NZIK;K')a^+_\gamma(F)a^+_\delta(F)$$

$$\times |Q'(F)\rangle f^{NZI}_{K'Q';1}(L^{-1})_{\delta\beta} = 0. \tag{6.6}$$

Together with the diagonalisation of H^{11} in the quasiparticle representation $\boldsymbol{F}$ (3.5), (3.6) and (6.6) are the variational equations of the MAD VAMPIR approach.

6.2. Numerical feasibility and possible achievements

The structure of the above variational equations is again very similar to those of the VAMPIR and EXCITED VAMPIR approaches. They can hence be handled using exactly the same numerical method as discussed in § 4.2. The only complication, which comes in, is the more general form of the energy functional and the gradient vector (6.6), the numerical evaluation of which becomes more time consuming. So for example the restriction of (6.1) to the projected one quasiparticle configurations alone already requires the calculation of the full projected one quasiparticle with three quasiparticle matrix in (6.6) and in case of the MONSTER(VAMPIR) configuration space (3.3) even the full two quasiparticle with four quasiparticle matrix would be needed. At present, at least in large single particle basis systems, the latter seems to be out of the range of the present computer facilities. For the case of complete one quasiparticle configuration spaces, however, the situation is different, at least if the same approximations as in § 4.3 are imposed. For this particular case the above equations have been thoroughly studied and first estimates show that their numerical evaluation should not require much more effort than for example the solution of the EXCITED VAMPIR problem. Thus we are rather confident that results of first realistic calculations with complete projected one quasiparticle configuration spaces will be available within the next few years.

This MAD VAMPIR approach with projected one quasiparticle configurations would close the most disappointing gap being left by all the other above discussed methods, namely their inability to describe odd mass nuclear systems on the same level of sophistication as the even ones. The method would produce optimised mean fields for odd systems at a given angular momentum. Thus, for example, backbending or

even more drastic changes in the structure of the yrast states become easily accessible and arbitrary changes of the mean fields as compared to those of the neighbouring even systems are incorporated.

Nevertheless, even the MAD VAMPIR description of odd nuclei still has a major deficiency. As already discussed for the MONSTER(VAMPIR) approach, also in the MAD VAMPIR the mean field is only adjusted to the yrast state of a particular spin value and thus again only the yrast structures themselves as well as structurally similar states are accessible. For the description of non-yrast states with completely different structures therefore also here, in analogy to the EXCITED VAMPIR approach for the even systems, a sort of EXCITED MAD VAMPIR scheme should be developed. However, such a generalisation, though rather straightforward, at the moment is only a vague speculation for the future and will hence not be discussed in the present article.

7. Conclusion

In the present article some recent developments have been reviewed, which allow us to perform microscopic nuclear structure calculations in large model spaces going far beyond the possibilities of a complete diagonalisation of the nuclear many body Hamiltonian. Several approaches have been discussed, which all 'parametrise' the nuclear wavefunctions by general HFB type quasiparticle configurations and leave the special form of the these quasiparticles as well as the configuration mixing degrees of freedom to be determined by variational procedures of increasing sophistication. In the most advanced of these approaches even the construction of the configuration space itself is left entirely to the dynamics of the considered system and determined by a chain of successive variational calculations. Thus here, at least in principle, the description of low lying nuclear excitations of arbitrary complexity has become numerically possible.

Being able to use general effective two body interactions in very large single particle basis systems these methods provide an up to now unique possibility for real 'large-scale' nuclear structure studies aiming at a unified description of the enormous multitude of experimental data all over the mass table. The essential presupposition for the achievement of this task is obviously the availability of suitable effective interactions for different mass regions and model spaces of various size. Unfortunately really 'good' effective forces have been designed only for the very small model spaces, in which complete SCM diagonalisations are possible. For the much larger basis systems we are interested in here, not much has been done up to now. This fact considerably handicaps the immediate application of these sophisticated methods to many interesting problems. Instead, for each new mass region and model space under consideration first time consuming systematic analyses have to be performed in order to obtain enough information about the necessary renormalisation of the many body Hamiltonian. On the other hand, though being rather tedious, such a procedure gives also the chance to get some quantitative insight into the properties of the nucleon-nucleon interaction inside the nucleus and thus should definitely be pursued further. Obviously, up to now only the first steps in this direction have been made. As discussed extensively in the present article, a couple of technical difficulties should still be overcome and many more systematic analyses in various mass regions will be needed before we can hope to pin down the 'egg or hen' problem of the effective interaction reasonably well. Nevertheless, we think that already the few realistic applications of these new methods,

available up to now, are extremely encouraging and support our hope that such a project cannot only be performed in principle but also in practice.

It has been argued lately that the really exciting developements in nuclear physics today are only taking place in the intermediate eneregy regime and that low energy nuclear spectroscopy hides no further surprises and should thus be left alone. We do not share this opinion. First of all, the rapid progress of both experimental as well as theoretical low energy nuclear physics within the last decade producing a lot of exciting new data and interpretations can hardly be overlooked. Furthermore, even with subnucleonic degrees of freedom and relativistic effects obviously being present in nuclei, valid conclusions about their real importance for low energy nuclear excitations require a sufficient mastery of the conventional nuclear many body problem in order to separate real effects from spurious deficiencies in the theoretical description. Last but not least, already today intermediate energy nuclear physics has been forced to leave simple single particle like interpretations and has become a many body problem as difficult if not more complex than that encountered in low energy nuclear physics. Thus the development of suitable effective many body theories will remain one of the central problems of modern physics irrespective of the particular energy regime. Whatever we can learn about it from experimental as well as theoretical investigations in the ideal testing ground of low energy nuclear spectroscopy with its multitude of various phenomena may also become rather valuable for other energy regions.

Acknowledgments

We both owe much to Amand Faessler, our common academic teacher and mentor for a long time. His continuous interest and continued encouraging support for our 'monstrous' projects are warmly appreciated. Credit should also be given to all the others who devoted much time and intelligence to turn frightening beasts into harmless little pets that are fun to play with: firstly Esko Hammaren, but also B Fladt, T Horibata, T Kaippinen, M Kyotoku, T Tomoda and Zheng Ren-Rong, without whom MONSTER and VAMPIR would not be what they are now. Finally countless discussions and invaluable suggestions by many of our other colleagues in Jülich and Tübingen are gratefully acknowledged as well as financial support from the Bundesministerium für Forschung and Technologie of the FRG.

References

Alberger D E 1984 *Nucl. Data Sheets* **42** 369-455
Arima A and Iachello F 1975a *Phys. Lett.* **57B** 39-43
—— 1975b *Phys. Rev. Lett.* **35** 1069-72
—— 1984 *Adv. Nucl. Phys.* **13** 139-200
Baranger M 1961 *Phys. Rev.* **122** 992
—— 1963a *Phys. Rev.* **130** 1244-52
—— 1963b *Cargese Lectures in Theoretical Physics* ed M Levy (New York: Benjamin)
Bardeen J, Cooper L N and Schrieffer J R 1957 *Phys. Rev.* **108** 1175
Bayman B F 1960 *Nucl. Phys.* **15** 33
Benczer-Koller N, Hass M and Sak J 1980 *Ann. Rev. Nucl. Part. Sci.* **30** 53-84
Bengtsson R and Frauendorf S 1979 *Nucl. Phys.* A **314** 27-36
Bloch C and Messiah A 1962 *Nucl. Phys.* **39** 95-106

Bogoliubov N N 1958 *Zh. Eksp. Teor. Fiz.* **34** 58
—— 1959 *Usp. Fiz. Nauk* **67** 541
Bogoliubov N N and Soloviev V G 1959 *Dokl. Akad. Nauk* **124** 1011
Bohr A and Mottelson B R 1969 *Nuclear Structure* vol 1 (New York: Benjamin)
Brodlie K W 1977 *The State of the Art in Numerical Analysis* ed D Jacobs (New York: Academic) p 229
Brussaard P J and Glaudemans P W M 1977 *Shell-Model Applications in Nuclear Spectroscopy* (Amsterdam: North-Holland)
Chung W 1976 *PhD thesis* Michigan State University
Decharge J and Gogny D 1980 *Phys. Rev.* C **21** 1568-93
Edmonds A R 1957 *Angular Momentum in Quantum Mechanics* (Princeton, NJ: Princeton University Press)
Egido J L, Mang H J and Ring P 1980 *Nucl. Phys.* A **334** 1-20
Emling H 1984 *Electromagnetic Properties of High-Spin Nuclear Levels. Annals of the Israel Physical Society* vol 7, ed G Goldring and M Hass (Bristol: Adam Hilger) pp 161-84
Fock A 1930 *Z. Phys.* **61** 126
Glaudemans P W M 1985 *Nuclear Structure at High Spin, Excitation, and Momentum Transfer* ed H Nann (New York: Am. Inst. Phys.) pp 316-26
Goldberg M B, Broude C, Dafni E, Gelberg A, Gerber J, Kumbartzki G J, Niv Y, Speidel K H and Zemel A 1980 *Phys. Lett.* **97B** 351-4
Griffioen R D and Sheline R K 1974 *Phys. Rev.* C **10** 624-31
Grümmer F, Schmid K W and Faessler A 1979 *Nucl. Phys.* A **326** 1-25
Halbert E, McGrory J B, Wildenthal B H and Pandhya S R 1971 *Adv. Nucl. Phys.* **4** 315-442
Hammaren E, Schmid K W, Faessler A and Grümmer F 1986a *Phys. Lett.* **171B** 347-52
Hammaren E, Schmid K W, Grümmer F, Faessler A and Fladt B 1985 *Nucl. Phys.* A **437** 1-46
—— 1986b *Nucl. Phys.* A **454** 301-37
Hanewinkel H, Gast W, Kaup V, Harter H, Dewald A, Gelberg A, Reinhardt R, von Brentano P, Zemel A, Alonso C E and Arias J M 1983 *Phys. Lett.* **133B** 9-12
Haque A M I *et al* 1985 *Capture Gamma-Ray Spectroscopy and Related Topics* (New York: Am. Inst. Phys.) pp 423-6
Hara K and Iwasaki S 1979 *Nucl. Phys.* A **332** 61-8
—— 1980 *Nucl. Phys.* A **348** 200-20
Hartree D R 1928 *Proc. Camb. Phil. Soc.* **24** 89
Heisenberg J and Blok H P 1983 *Ann. Rev. Nucl. Part. Sci.* **33** 569-609
Hill D L and Wheeler J A 1953 *Phys. Rev.* **89** 1102
Holinde K, Erkelenz K and Alzetta R 1972 *Nucl. Phys.* A **194** 161-76
Kelson I 1963 *Phys. Rev.* **132** 2189-93
Kocher D C 1976 *Nucl. Data Sheets* **17** 39-95
Kowalik J and Osborne M R 1968 *Methods for Unconstrained Optimization Problems* (Amsterdam: Elsevier)
Kuo T T S and Brown G E 1968 *Nucl. Phys.* A **114** 241-79
Kumar K and Baranger M 1968 *Nucl. Phys.* A **110** 529-54
Lieder R M, Jäger H, Neskakis A, Venkova T and Michel C 1984 *Nucl. Instrum. Methods* **220** 363-70
Mang H J 1975 *Phys. Rep.* **18** 325-68
Mang H J, Samadi B and Ring P 1976 *Z. Phys.* A **279** 325-9
McGrory J B 1973 *Phys. Rev.* C **8** 693-710
McGrory J B and Wildenthal B H 1980 *Ann. Rev. Nucl. Part. Sci.* **30** 383-436
Neergard K and Wüst E 1983 *Nucl. Phys.* A **402** 311-21
Onishi N and Yoshida S 1966 *Nucl. Phys.* **80** 367-76
Peierls R E and Yoccoz I 1957 *Proc. Phys. Soc.* A **70** 381
Ring P and Schuck P 1980 *The Nuclear Many-Body Problem* (Berlin: Springer)
Ripka G 1968 *Adv. Nucl. Phys.* **1** 183-259
Schiffer K, Dewald A, Gelberg A, Reinhardt R, Zell K O, von Brentano P and Sun Xiangfu 1983 *Z. Phys.* A **313** 245-6
Schmid K W 1981 *Phys. Rev.* C **24** 1283-321
Schmid K W and DoDang G 1977 *Phys. Rev.* C **15** 1515-29
—— 1978 *Phys. Rev.* C **18** 1003-10
Schmid K W and Grümmer F 1979 *Z. Phys.* A **292** 15-26
Schmid K W, Grümmer F and Faessler A 1984a *Phys. Rev.* C **29** 291-307
—— 1984b *Phys. Rev.* C **29** 308-23
—— 1984c *Nucl. Phys.* A **431** 205-29

Schmid K W, Grümmer F, Hammaren E and Faessler A 1985 *Nucl. Phys.* A **436** 417-37
Schmid K W, Grümmer F, Hammaren E, Kyotoku M and Faessler A 1986a *Nucl. Phys.* A **456** 437-56
Schmid K W, Grümmer F, Kyotoku M and Faessler A 1986b *Nucl. Phys.* A **452** 493-512
Stephens F S 1985 *Nuclear Structure* ed R Broglia, G Hagemann and B Herkind (Amsterdam: North-Holland) p 363
Stephens F S and Simon R S 1972 *Nucl. Phys.* A **183** 257-84
Thouless D J 1960 *Nucl. Phys.* **21** 225
Todd D M, Aryaeinejad R, Love D J G, Nelson A H, Nolan P J, Smith P J and Twin P J 1984 *J. Phys. G: Nucl. Phys.* **10** 1407-33
Twin P J, Nolan P J, Aryaeinejad R, Love D J G, Nelson A H and Kirwan A 1984 *Nucl. Phys.* A **409** 343c-51c
Twin P J *et al* 1986 *Phys. Rev. Lett.* **57** 811-14
Valatin J G 1961 *Phys. Rev.* **122** 1012
Villars F 1966 *Varenna Lectures* vol 36, ed C Bloch (New York: Academic) pp 1-42
Whitehead R R, Watt A, Cole B J and Morrison I 1977 *Adv. Nucl. Phys.* **9** 123-76
Wick G C 1950 *Phys. Rev.* **80** 268
Wilkinson J H 1965 *The Algebraic Eigenvalue Problem* (Oxford: Clarendon)
Yates S W *et al* 1980 *Phys. Rev.* C **21** 2366-84
Zeh H D 1965 *Z. Phys.* **188** 361
—— 1967 *Z. Phys.* **202** 38
Zemel A, Broude C, Dafni E, Gelberg A, Goldberg M B, Gerber J, Jumbartzki G J and Speidel K H 1982 *Nucl. Phys.* A **383** 165-88
Zumino B 1962 *J. Math. Phys.* **3** 1055